Damanhour Journal of Veterinary Sciences 13 (2), (2025) 27-54

Damanhour Journal of Veterinary Sciences

Journal homepage: https://djvs.journals.ekb.eg/

E-ISSN 2636-3003 | ISSN 2636-3011

Ameliorative effect of Silymarin nano collagen preparation on Aluminum chloride induced Alzheimer disease in rat model

Lamiaa G. Wasef[1], Amany M. Alama[2], Manal Aly Shalaby[3], Rehab Mady[1] Gaber El-Saber Batiha[1], and Hazem M. Shaheen[1*]

1Department of Pharmacology and Therapeutics, Faculty of Veterinary Medicine, Damanhour University, Damanhour 22511, Damanhour, Egypt;

2 Inspection department on the campus and butcher shops ,

3Department of Medical Biotechnology, Institute of Genetic Engineering City of Scientific Research and Biotechnological Applications ,Egypt.

Abstract:

Silymarin, a flavonoid derived from plants, has emerged as a potential neuroprotective agent against Multiple neurological conditions, as Alzheimer's disease (AD), cerebral ischemia, and Parkinson's disease. Fish-scale collagen, known for its high biodegradability, excellent biocompatibility, and low antigenicity, was utilized in this study to create collagen nanoparticles for neuroprotection drug delivery. The investigation aimed to extract Mullet scale-derived collagen and produce collagen nanoparticles using ethanol as an insoluble solvent. Silymarin Was incorporated into the nanoparticles via the nanoparticle precipitation method. MTT assay was employed to compare the cytotoxicity of Collagen nanoparticles loaded with silymarin with that of free silymarin. Remarkably, no statistically significant change in cytotoxicity was observed in cells that have been served by silymarin rates lower than 100 µg/ml. The study successfully demonstrated the effective loading of silymarin into collagen nanoparticles, these findings were confirmed by transmission electron microscopy (TEM) and dynamic light scattering (DLS) ,(TEM), technique on a Zeta sizer Nano ZS, scanning electron microscope, also FTIR is used for measuring the radiation absorption of infrared regions at various wavelengths. Notably, the cytotoxic effects of silymarin followed a consistent pattern at all concentrations: silymarin loading in collagen nanoparticles < silymarin nanoparticles < free silymarin. Also, we demonstrate the therapeutic impact of silymarin nanoparticle and collagen nanoparticle on antioxidant biomarkers in brain tissues of AlCl3 induced Alzheimer's that that confirmed by the histological analysis of the brain that show substantial neuroprotective of silymarin plus collagen nanoparticles, this suggests that loading silymarin into collagen nanoparticles is both efficient and safe.

Keywords: *Characterization; Cytotoxicity; Behavioral; Oxidative; Antioxidant*

[*]Correspondence: **Hazem M. Shaheen[1*]**

1Department of Pharmacology and Therapeutics, Faculty of Veterinary Medicine, Damanhour University, Damanhour 22511, Damanhour, Egypt .

Email: **dr_hazemshaheen3010@yahoo.com;**

P ISSN: 2636-3003
EISSN: 2636-2996
DOI: 10.21608/djvs.2025.385719.1156
Received: May 26, 2025; Received in revised form: July 23, 2025; accepted: September 30, 2025
Editor-in-Chief: Ass. Prof .Dr/Abdelwahab A. Alsenosy (editor@vetmed.dmu.edu.eg)

1. Introduction

Silymarin is a compound of flavones derived from lignin, with Silybum (constituting the majority), with lesser amounts of silydianin and isosilybin. It was initially identified as a combination made from the extract of the seed Silybum Marianum in 1968. Following that, each component was purified, and methods like X-ray crystallography and NMR for clarifying their structures.**(N. Karim et al., 2020)** . The neuroprotective effects of Silymarin have been validated in cellular models of Alzheimer's disease (AD) involving both neuronal and non-neuronal cells, including moderate cognitive impairment (CI) and Parkinson's disease (PD) **(Cordaro, Cuzzocrea, & Crupi, 2020).** The same effects have been observed in animal models representing various neurodegenerative conditions. The studies encompassed investigations into the appropriate dosages for ttreatment applied in both *in vitro* and *in vivo* experiments, the application schedules, the formulations employed, and the duration of Silymarin treatment **(Usman et al., 2009).**

Alzheimer's disease (AD) is a rapidly developing disease; it is anticipated that approximately 70 million individuals will be impacted by 2030, with this figure likely to increase by 115 million by 2050 **(Liza, Roy, Iktidar, Chowdhury, & Sharif, 2024)**. Adults in their middle to late years are the main victims of AD, an age-related, complex, progressive neurological disease. In the early AD stages, intermittent memory loss is a conspicuous symptom ,significantly impair an individual's ability to perform daily living activities progressive cognitive decline and behavioral and functional changes **(Ferrer, 2022; Gamache, Yun, & Chiba-Falek, 2020).** The most frequent sign of AD is persistent memory loss, even when many managerial purposes, as attention, language, direction, and judgement, are impaired **(Chiu et al., 2004).** Reports on Silymarin's effects on other oxidative stress-related central nervous system disorders, like Huntington's disease, multiple sclerosis, and amyotrophic lateral sclerosis, are noticeably lacking **(Haddadi, Shahidi, & Eyvari-Brooshghalan, 2020; Mayer, Veronikas, & Shaughnessy, 2005).** Additional research and investigation into these particular neurological disorders may yield important information about the possible wider neuroprotective benefits of silymarin outside of AD and PD.

Collagen nanoparticles represent a type of polymeric nanoparticle extensively employed in drug delivery systems. **(Begines et al., 2020; Lo & Fauzi, 2021; Sahithi et al., 2013)** .In recent researches , collagen was extracted from mullet scales using the dissolution method, leading to the formation of nanoparticles. Subsequently, these collagen nanoparticles were utilized to load silymarin, a process not only innovative but also potent. In the context of our study, collagen was chosen due to its inherent advantages, for example, it is a natural compound that is biocompatible with humans, biodegradable, and does not trigger allergic responses **(Jafari et al., 2020).**

Aluminum chloride has been identified as a strong neurotoxin and linked to Alzheimer's disease due to its role in worsening oxidative damage in the brain, caused neural damage, and induced Aβ deposition, which leaded to diminishing in memory **(Kawahara, Tanaka, & Kato-Negishi, 2021).** It led to impaired glucose utilization, elevated free radical production, and lipid peroxidation, along with alterations in phosphoinositide metabolism and protein phosphorylation, resulting in severe neurotoxicity. Moreover, the reduction in the activities of lipid peroxidase, nitric oxide synthase, and acetylcholinesterase helped prevent the aggregation of amyloid β, a key characteristic of neurodegenerative disorders **(Aboelwafa, El-Kott, Abd-Ella, & Yousef, 2020).**

Our study looks at how collagen nanoparticles loaded with silymarin affect cell survival. Also explains the impact of silymarin nanoparticle and collagen nanoparticle on some antioxidant markers and Histopathological studies on brain and hippocampus in brain tissues of AlCl3 induced Alzheimer's. This approach aligns with the growing interest in utilizing collagen-based nanocarriers for drug delivery, capitalizing on collagen's biocompatibility and potential for controlled release of Therapeutics.

2. Materials and methods

2.1. Chemicals:

In this study, silymarin was obtained from Sigma Aldrich Chemical Company (St. Louis, MO, USA). Mullet fish scales were sourced from a local market in the Egyptian governorate of

Beheira. Glutaraldehyde, sodium hydroxide, acetic acid, and ethanol were acquired from Merck Co. in Germany. All chemicals and solvents employed in this investigation were of high purity and HPLC-grade, respectively. Additionally, Chemicals and experimental Components for establishing cell lines and conducting cell cultures were procured from Merck Co., Germany. The reagents thiazolyl blue and dimethyl sulfoxide (DMSO) were purchased from Sigma-Aldrich, UK. The selection of chemicals, materials, reagents, and solvents from reputable sources aimed to ensure their superior quality in the research process.

2.2. Methods:

The experimental procedures were authorized by the Institutional Animal Ethics Committee of the Faculty of Veterinary Medicine, Damanhour University under all hygienic conditions using recoded published methods **(Approval Number: DMU/VetMed-2025/013).**

2.2.1. Collagen Extraction from fish scales

The grey mullet scales were manually collected and then cleaned thoroughly using Purified water Subsequently, the samples dehydrated, placed in polybags, and stored at 25 °C until ready for use. Collagen extraction was performed with slight modifications to the standard protocol ,following the procedure outlined by **(Shalaby et al., 2020).** In order to purify the fish scales, pigments and non-collagenous proteins were eliminated, they were subjected to a 0.1N NaOH solution maintained for two days before then washed with distilled water. After a two-day treatment with a 0.50 M acetic acid solution, the samples were homogenized for three hours. The resulting solution was filtered after the removal of supernatants**.**

2.2.2. Synthesis of collagen nanoparticles and loading of the drug

Collagen nanoparticles were produced using the nanoprecipitation method, specifically employing ethanol, as described by **(Solanki & Patel, 2024).**Ethanol was introduced into the solution through a burette with free flow while stirring, led to protein unfolding and a conformational shift in collagen from a stretched to a coiled state .Silymarin was dissolved in ethanol and stirred maintained at 100 °C for one hour. The resulting formulation was mixed with collagen nanoparticles by passing it through a strainer, ensuring thorough mixing over the course of an hour. Stirring, in conjunction with glutaraldehyde, was then used to induce particle cross-linking. **2.3. Characterization and Analysis of Collagen Nanoparticles and Drug Encapsulation**

The nano formulations were morphology and size Analyzed by transmission electron microscopy (TEM). (TALOS Instrument, Thermo Fischer Scientific, United States) at SRTA-City, Egypt, Dynamic light scattering (DLS) analysis was performed using a Zetasizer Nano ZS (Malvern Instruments Corp)., Malvern, United Kingdom), scanning electron microscope (S-4800, Hitachi, Japan). also, FTIR is used for measuring the radiation absorption of infrared regions at various wavelengths were obtained on a Shimadzu FTIR-8400S (Tokyo, Japan).

2.4 Experimental Strategy

A total of forty-two albino rats were grouped into six groups each of 7 rats, acquired from the animal house in the faculty of medicine, Alexandria University **Group I:** (Control negative group): which was injected intraperitoneally, i.p. with physiological saline 0.2 ml/day for 15 days. **Group II** (AlCl3 group): rats intraperitoneally injected with (AlCl3) administered at 100 mg per kg per day for 15 consecutive days. **(Mathiyazahan;2015). Group III** (AlCl3+ SM group): rats daily injected with (200 mg/kg /day) SM suspended in 1 mL corn oil (vehicle) for 15 days using oral gavage **(Galhardi ; 2009**), concomitant with AlCl3 100 mg/kg/day for 15 days in the same manner. **Group IV** (AlCl3 + Collagen group): rats were given 100 mg/kg/day collagen concomitant with 100 mg/kg/day AlCl3 for 15 days in the same manner. **Group V** (AlCl3+ SM nano group): rats orally administrated (200 mg/kg/day) SM nanoparticles were dispersed in 1 mL of corn oil which used as the vehicle. concomitant with 100 mg/kg/day AlCl3 for 15 days in the same manner. Group **VI** (AlCl3+ SM loaded collagen nano group, rats orally administrated (200 mg/kg) M collagen nanoparticles were dispersed in 1 mL of corn oil as the vehicle. with 100 mg/kg/day AlCl3 for 15 days.

2.5. Cell culture and cytotoxicity examining

Cell viability was measured using the MTT (3-(4,5-dimethylthiazol-2-yl)-2,5-diphenyltetrazolium bromide) on WI-38 lung normal cells delivered by the NCCS in Pune, India. The procedure was executed in 2mL microtubes in accordance with the procedure delineated by (**Farias et al., 2013)** with certain improvements. Initially Serial duplicated dilutions of each derivative were made using 0.9% NaCl, with concentrations varying between 1.0 and 1.9 µg/mL. Afterwards, 100 µL of A mixture comprising 1% red blood cells derived from rabbit blood or human blood types A, B, and O was added to a fresh microtube holding 900 µL. of each diluted extract. This mixture was incubated at 37°C for one hour in an incubator. Afterward, the samples were spun at 3,000 g in a centrifuge for a duration of five minutes. The upper phase (200μL) was transferred to a 96-well plate connected to a microplate reader, and the absorbance at 540 nm was determined. To determine baseline values for 100% and 0% cell lysis, 100 µL of each human blood type or rabbit red blood cell suspension was combined with either distilled water or 0.9% NaCl (900 µL) respectively. The fraction of hemolysis was determined using the following formula: Percentage hemolysis = (Abs test/Abs pb) × 100, where Abs test represents the Abs540 of the 1% cell suspension treated with the test sample, and Abs pb corresponds to the absorbance (540 nm) of the 1% cell mixture after treatment with distilled water. To determine the correlation between extract concentration and hemolysis percentage, Hemolysis was evaluated as the minimum seed extract ratio (μg/mL) inducing hemolysis equal to or greater than 50%. Each perseverance test was conducted in triplicate.

2.6. Behavioral tests:

These tests were performed after 15 consecutive days of treatment to validate impairments induced in injected rats (groups III, IV, V and VI) against negative controls (group I and II).

2.6.1. Inhibitory avoidance test

The apparatus consists of a double-compartment light/dark shuttle box. During the acquisition trial, an electric shock (75 V, 0.2 mA, 50 Hz) is delivered for 5 seconds immediately after the rat enters the dark chamber. The first entry latency into the dark compartment was noted during the acquisition phase. After 5 seconds in the dark chamber, each rat was returned to its original cage. Retention latency was assessed 20 hours later in a trial identical to the acquisition phase but without foot shock. The period required to reach the dark compartment (retention latency) was measured, with 300 seconds as the upper limit. Memory impairment was indicated by shorter latencies to enter the dark compartment, whereas significantly longer latencies reflected better memory retention. Rats that did not enter the dark chamber within the test period were assigned a maximum score of 300 seconds **(Sakurai et al., 2008)**

2.6.2. Water maze test

Learning and memory preservation were assessed using the Morris water maze test. The apparatus consisted of a large circular pool (120 cm in diameter, 48 cm in height) filled to a depth of 30 cm with water maintained at 28 ± 1 °C. The pool was visually divided into four equal quadrants using two intersecting threads positioned at right angles. The pool was located in a well-lit room containing several colored visual cues, which remained constant throughout the experiment and served as spatial reference points for memory assessment. During the acquisition phase, a circular platform (4.5 cm in diameter) was positioned in one of the quadrants, 1 cm above the water surface. For the retention phase, the same platform was submerged 1 cm below the water level. The platform position remained fixed within the same quadrant throughout both the acquisition and retention phases. Each rat underwent four consecutive trials, with a 5-minute interval between trials. For each trial, the animal was gently placed into the water at varying drop points between quadrants, facing the pool wall. The animal was given up to 120 seconds to find the hidden platform. After locating the platform,

the animal was permitted to remain on it for 20 seconds. If the animal was unable to locate the platform within 120 seconds, it was mildly guided to the platform and permitted to stay there for the same duration. **(Mahapatra et al., 2020; Sathya et al., 2018).**

2.7. Tissue Preparation

Following the exploratory phase, the animals were anesthetized using diethyl ether. The entire brains were then carefully removed on an ice-cold surface and rinsed with ice-cold isotonic physiological saline. Next, the brains were split into right and left hemispheres using a sharp blade to isolate the hippocampi. Hippocampal tissues from four randomly selected brains were processed for histological and ultrastructural analysis, while the weighed hippocampi from the remaining brains were homogenized in ice-cold 0.1 mmol/L PBS (pH 7.4) using a Teflon-glass homogenizer. The homogenates (10%, w/v) were centrifuged at 10,000 rpm for 15 minutes, and the resulting supernatants were stored at -80°C for later biochemical analyses.

2.7.1. Biochemical analysis (Oxidative parameter and Antioxidant parameter)

The extent of lipid peroxidation was evaluated by determining Thiobarbituric Acid Reactive Substances (TBARS) levels in the homogenate. **(Chen & Tappel, 1996)** , Nitric in the homogenate was determined according to **(Montgomery, Dymock, & Thom, 1962)** ,Determination of homogenate reduced glutathione (GSH) level by **(Bielawski & Joy, 1986) ,**Determination of homogenate catalase assay **(Drotar, Phelps, & Fall, 1985)** and determination of brain homogenate superoxide dismutase (SOD) **(Nandi & Chatterjee, 1988)**

2.7.2. Histopathological examination

Following complete necropsy of treated and control rats. The hippocampi from all rats were cut into small segments and fixed in Bouin's solution for 24 hours. Following the previously described protocol, all hippocampal samples were sent for paraffin sectioning. Paraffin sections, 4–6 µm thick, were then stained with Ehrlich's hematoxylin and eosin (H&E). After staining, the sections were dehydrated through a series of graded ethanol concentrations, cleared in xylene, mounted with DPX, and examined under a BX-40 Olympus compound light microscope equipped with a Panasonic CD camera, where they were photographed. **(Meyerholz & Beck, 2018)**

2.8. Statistical analysis

Results are presented as the mean ± standard error of the mean (SEM). Statistical analysis of the results was performed using one-way analysis of variance (ANOVA). Significant differences between means were further analyzed using Tukey's post-hoc multiple comparison test, with significance set at $P < 0.05$.

Results*3.1. Dynamic light scattering (Zeta sizer)*

silymarin

The size distribution graph shows a single prominent peak at 1063 nm, with 100% intensity, The standard deviation of 169.3 nm suggests a relatively wide distribution around the main peak size. The intercept value of 0. (**figure1).**

Fish scale-based collagen-silymarin nanoparticles

The results show that the nanoparticles have a typical size of about 346.5 nm in diameter, as indicated by the Z-Average. The size distribution peaks at 374.9 nm, with a smaller peak at 5126 nm, The polydispersity index (PdI) of 0.255, distribution graph shows a primary peak around 374.9 nm, with a high intercept value of 0.955 **(figure 2).**

The silymarin nanoparticles

The Z-Average diameter is approximately 501.7 nm, The polydispersity index (PdI) was measured at 0.661. the first peak at 268.5 nm with 67.4% intensity, the second peak at 1052 nm with 29.0% intensity, and the third peak at 5510 nm with 3.6% intensity, the intercept value of 0.900 indicates good reliability of the measurements, and the result quality is marked as "Good," **(Figure 3)**

3.2. TEM Analysis and EDX mapping

The transmission electron microscopy (TEM) images illustrate the morphology of Silymarin powder Figure 4A, collagen-based nanoparticles

Figure 4B and Silymarin based particles. The images demonstrate uniformity in shape and size distribution, supporting the effectiveness of the nanoparticle preparation method **(Figure 4).**

3. Scanning Electron Microscopy

The scanning electron microscope (SEM) image figure 5A shows silymarin particles at a magnification of X20,000. The particles are spherical in shape and exhibit smooth surfaces,

The scanning electron microscope (SEM) image figure 5A provides detailed visualization of silymarin-based nanoparticles at high magnification (X10,000).

4. Fourier Transform Infrared (FT-IR) Spectral Analysis

FTIR spectrum of collagen (figure 8) reveals several characteristic peaks indicative of collagen's molecular structure.

Impact of silymarin on FTIR **(figure 7)**: observed peak value of a CO-H stretching presence at 3000 cm-1, 1510.81 cm-1 and 922.58 cm-1 respectively representing alkene and ketone.

The spectrum of the silymarin collagen nanoparticle **(figure 10)** showed bands for amide I at 3315.09 cm− 1, amide II at 2977.28 cm− 1, amide III at 1638.65 cm− 1.

The spectrum of the silymarin nanoparticle **(figure 9)** showed bands for amide I at 3432.70 cm− 1, amide II at 2936.32 cm− 1, amide III at 1726.44 cm− 1.

Figure 15 FTIR spectrum of the silymarin-collagen loaded nanoparticles exhibit a peak at 2977.28 cm^{-1}, which corresponds to C-H stretching vibrations, which are characteristic of the aliphatic chains in both silymarin and collagen. This peak further supports the presence of these two compounds in the nanoparticles.

3.2- In vitro Drug Release Study

Controlled release under in vitro conditions profiles of free silymarin and silymarin-loaded nanoparticles were monitored over a 48-hour period for both formulations. Within the first 10 hours, approximately 126.32 ± 0.01% of the drug was released from the silymarin nanoparticles, compared to 160.00 ± 0.03% release from the free drug. The release kinetics demonstrated that silymarin nanoparticles exhibited a slower and more controlled release into phosphate buffer at physiological pH 7.4 compared to the free silymarin released under the same conditions.

3.2.1. Cell culture and cytotoxicity examining

The graph compares the cytotoxicity of Silymarin in tablet form versus Silymarin in nanoparticle form by showing cell viability percentages across a range of concentrations. As the concentration decreases from 500 µg/mL to 15.6 µg/mL, cell viability for both forms of Silymarin increases, indicating that lower concentrations are less toxic to the cells. This trend is consistent for both Silymarin tablets and nanoparticles, demonstrating a concentration-dependent relationship in cytotoxicity. For Silymarin tablets, the IC50 is around 125 µg/mL, meaning that at this concentration, cell viability is reduced to 50%. In contrast, the IC50 for Silymarin nanoparticles is significantly higher, likely around 500 µg/mL or more. This higher IC50 value indicates that a greater concentration of nanoparticles is required to achieve the same level of cytotoxicity observed with the tablets (**Figure 11).**

3.2.2 Hemolysis assay to test cytotoxicity

The graph illustrates the haemolysis assay results for Silymarin in tablet form and Silymarin in nanoparticle form, showing the relationship between concentration (µg/mL) and haemolysis percentage. homolysis is a measure of cytotoxicity to red blood cells, with higher percentages indicating greater cell membrane damage (Figure 12).

For both Silymarin tablets and nanoparticles, the haemolysis percentage increases gradually as the concentration increases from 10 µg/mL to 40 µg/ml.

At lower concentrations, both Silymarin tablets and nanoparticles exhibit similar levels of haemolysis, with the percentage remaining relatively low and close to each other. As the concentration increases, the haemolysis percentage for Silymarin nanoparticles tends to rise more sharply compared to the tablets,

especially at the higher concentrations. For instance, at 40 µg/mL, Silymarin nanoparticles show a higher haemolysis percentage than the tablets, indicating that nanoparticles may cause more damage to red blood cells at these higher concentrations.

3.3. Behavioral observations

3.3.1. Passive avoidance test

In the control negative group, the slowest rat took 12 seconds to enter the shock area, while the fastest rat took 40 seconds. This range indicates normal variability in response times within a healthy population, For the control positive group exposed to AlCl3, the slowest rat entered the shock area in 10 seconds, and the fastest in 37 seconds. These shorter times suggest a significant impairment in memory retention and learning due to AlCl3 exposure. Rats receiving silymarin treatment exhibited better performance. compared to the AlCl3 group. The slowest rat took 11 seconds, and the fastest rat took 40 seconds to enter the shock area. In the collagen-treated group, the slowest rat entered the shock area in 15 seconds, while the fastest took 46 seconds. The group treated with silymarin nanoparticles exhibited a significant improvement, with the slowest rat taking 9 seconds and the fastest 33 seconds to enter the shock area. This group shows a narrower range of times. The silymarin collagen nanoparticles group demonstrated the best performance. The slowest rat took 11 seconds, while the fastest rat took only 22 seconds to enter the shock area. This narrow range indicates high efficacy in memory retention and learning, with the majority of the rats remembering to avoid the aversive stimulus. The results closely resemble the control negative group's performance, highlighting the superior neuroprotective effects of the combined nanoparticle treatment.

The results in ***Table 1*** showed comparison between control and all treated groups in passive avoidance test. A widely used behavioral test for evaluating learning and memory in rodents. It involves training the animals to avoid an aversive stimulus, typically a mild foot shock, by remembering the environment where the shock was administered.

3.3.2. Water maze test

(Group I) In the control negative group, the rats took an average of 9.6 seconds to find the platform, traveling a distance of 120 cm at a speed of 12.5 cm/s. (Group II) group which exposed to AlCl3, exhibited significant impairment. The rats took 3.5 seconds to locate the platform, covering the same distance of 120 cm but at a much higher speed of 34.2 cm/s. Rats treated with silymarin took 7.3 seconds to find the platform, with a distance of 120 cm and a speed of 16.4 cm/s. This group demonstrated better performance than the ALCL3 treated group. In the collagen-treated group, rats took 10 seconds to locate the platform, traveling 120 cm at a speed of 12 cm/s. The time taken is longer compared to the control negative group, indicating that collagen alone does not significantly enhance cognitive performance. Rats treated with silymarin nanoparticles took 9 seconds to find the platform, with a distance of 120 cm and a speed of 13.3 cm/s. This group performed better than the control positive and silymarin groups, showing that the nanoparticle formulation enhances the cognitive benefits of silymarin, likely due to improved bioavailability. The silymarin collagen nanoparticles group exhibited near-normal performance, taking 9.5 seconds to find the platform, traveling 120 cm at a speed of 12.6 cm/s. This group's performance is closest to the control negative group, indicating that the combined treatment in nanoparticle form provides the most substantial neuroprotective and cognitive benefits, effectively mitigating the adverse effects of AlCl3.Figure (13) show comparison between control and all treated groups in water maze test. In this evaluation, the performance of different treatment groups was compared based on their time to locate the platform (time in seconds), the distance traveled (distance in centimeters), and their speed (speed in cm/s).

3.4. In vivo Studies Results

3.4.1. Biochemical Analysis (oxidative stress marker)

The therapeutic impact of silymarin nanoparticle and collagen nanoparticle on Indicators of antioxidant activity in brain tissues of ALCL3 induced Alzheimer's and different experimental groups

A - Results of Thiobarbituric Acid Reactive Substances (TBARS) expressed as μmol per gram of protein

The results are expressed as mean ± SE ($p<0.05$). Comparing the AlCl3-induced group with the treatment groups, the silymarin-treated group exhibited a TBARS level (0.58±0.04) μmol/g slightly lower than the AlCl3 group (1.51 ± 0.02) μmol/g but the difference was not statistically significant ($P < 0.05$), suggesting limited improvement in oxidative stress. In contrast, the collagen-treated group had a TBARS level (0.68 ± 0.04) μmol/g, which was lower than the AlCl3 group. The silymarin nanoparticle-treated group showed a TBARS level (0.77±0.11) μmol/g , lower than the AlCl3 group. The silymarin plus collagen nanoparticle-treated group had a TBARS level (0.85 ± 0.01) μmol/g, lower than the AlCl3 group and showing a moderate reduction compared to the silymarin nanoparticle group alone (Figure14)

b- Estimation of Nitric Oxide (No) Level (μm /G Protein)

The control group exhibited an NO level of (34.91 ± 1.31) μM/g, in contrast, the AlCl3-induced group showed a significantly increased NO level of (62.44 ± 1.31) μM/g. Relative to the AlCl3-induced group with the treatment groups, the silymarin-treated group demonstrated an NO level of (32.70±1.8) μM, which was slightly lower than the AlCl3-induced group and significantly different ($p<0.05$). The collagen-treated group showed a further decrease in NO level to (36.18 ± 1.80) μM, suggesting a more effective reduction of oxidative stress compared to silymarin alone. The silymarin nanoparticle-treated group exhibited a notably higher NO level of (47.00±9.62) μM, ($p<0.05$) higher than both silymarin group and other treatment groups. The group treated with silymarin plus collagen nanoparticles had an NO level of (35.07 ± 1.22) μM, slightly lower than the silymarin nanoparticles treated group though, It exhibited a significant change ($p < 0.05$) compared to the AlCl3 group. (Figure15)

C- Estimation Of Reduced Glutathione (GSH) Level (Mmol/G Protein)

The control group exhibited a GSH level of (14.44±0.58) μmol/g , while the AlCl3-induced rats displayed a significantly ($p<0.05$) lower GSH level of (13.36±0.71) μmol/g. Relative to the AlCl3-induced group with the treatment groups, the silymarin-treated group had a GSH level of (14.69±0.14) μmol/g. This level was higher than the AlCl3-induced group However, the variation was not significant when compared with the control group. ($p<0.05$). Similarly, the collagen-treated group had a GSH level of (19.03±3.89) μmol/g, showing higher than the silymarin-treated group, with an improvement in antioxidant status but not a complete normalization to control levels. The silymarin nanoparticle-treated group exhibited the highest GSH level of (25.52±0.39) μmol/g among all groups. The group treated with silymarin plus collagen nanoparticles had a GSH level of (14.64 ± 0.29) μmol/g , close to that of the silymarin treated groups, suggested a synergistic effect but without the extreme increased seen in the silymarin nanoparticle group (Figure 16)

Estimation of Catalase Level (U/Mg Protein)

The control group exhibited a catalase level of (62.33±1.45) U/mg protein, representing baseline antioxidant enzyme activity under normal conditions. In contrast, the AlCl3-induced group showed a significantly ($p<0.05$) lower catalase level of (59.67±3.18) U/mg protein. Relative to the AlCl3-induced group with the treatment groups, the silymarin-treated group demonstrated a catalase level of (65.33±0.88) U/mg protein. This level was comparable to that of the control group. The collagen-treated group showed a significant improvement ($p<0.05$) than control group with a catalase level of (84.33±17.27) U/mg protein. The silymarin nanoparticle-treated group exhibited the highest catalase level among all groups at (114.33 ± 1.76) U/mg protein, indicating a pronounced increase. The group treated with silymarin plus collagen nanoparticles had a catalase level of (65.00 ± 1.15) U/mg protein, similar to the silymarin-treated group, suggested a synergistic effect but without the extreme elevation seen in the silymarin nanoparticle group alone (Figure 17).

e- Estimation of glutathione peroxidase (GPx) level (U/mg protein)

The control group exhibited a GPx level of (20.18±1.39) U/mg protein, representing baseline antioxidant enzyme activity under normal conditions. In contrast, The $AlCl_3$-induced group exhibited a significantly ($p<0.05$) lower GPx level of (7.59±0.51) U/mg protein. Relative to the AlCl3-induced group with the treatment groups, the silymarin-treated group demonstrated a significantly increase GPx level compared to the AlCl3-induced group (20.96±1.36) U/mg protein, which was similar to control group. The collagen-treated group also exhibited a similar GPx level of (20.84±2.75) U/mg protein. The silymarin nanoparticle-treated group exhibited the highest GPx level among all groups at (29.10±1.47) U/mg protein. The group treated with silymarin plus collagen nanoparticles had a GPx level of (21.47±1.90) U/mg protein, which was lower than the silymarin nanoparticles group. (Figure18)

f- Estimation of superoxide dismutase (SOD) level (U/mg protein)

The control group exhibited an SOD level of (0.70 ± 0.04) U/mg protein, representing baseline antioxidant enzyme activity under normal conditions. In contrast, the AlCl3-induced group displayed a significantly ($p<0.05$) decrease SOD level of (0.60 ± 0.10) U/mg protein. Relative to the AlCl3-induced group with the treatment groups, the silymarin-treated group demonstrated an SOD level of (1.11±0.10) U/mg protein, which was significantly($p<0.05$) higher than the AlCl3 group and the control group. The collagen-treated group presented an SOD level of (0.90±0.10) U/mg protein, which was markedly ($p < 0.05$) elevated relative to both the control and $AlCl_3$-treated groups. The silymarin nanoparticle-treated group exhibited the highest SOD level among all groups at (1.21±0.15) U/mg protein, indicating a pronounced SOD increase. The group treated with silymarin plus collagen nanoparticles had an SOD level of (0.78±0.03) U/mg protein, which not significant difference as compared with control, suggesting synergistic effect of improvement in oxidative stress management (Figure 19)

3.4.2. Histopathological Assessment

The histological section of brain tissue treated with aluminium chloride (AlCl3) show morphological change in neurons (shrunken and irregularly shaped) that indicate impaired neuronal function and viability. neurodegenerative conditions, neurons exhibit intracytoplasmic inclusions, which are abnormal accumulations of proteins or other cellular components within the cytoplasm, noticeable reduction in neuronal density (Figure 22). The neurons in the hippocampus appear shrunken and irregularly shaped, reflecting significant cellular damage with severe cellular degeneration and cytoplasmic disintegration, there is extensive vacuolation within the neurons and the surrounding neuropil. The presence of vacuoles is often associated with the breakdown of cellular organelles and loss of cytoplasmic integrity. The section also reveals a noticeable reduction in neuronal density (Figure 23), The histological section of the hippocampus from rats induced with aluminium chloride (AlCl3) and treated with silymarin, reveals important insights into the Neuroprotective properties of silymarin in counteracting $AlCl_3$-induced neurotoxicity. that observed by apparent mitigation of neuronal damage. reduction in gliosis and improvement in neuronal density within the hippocampus (Figure 24,25). The histological section of brain tissue illustrates significant findings related to aluminum chloride (AlCl3) toxicity and subsequent treatment with collagen nanoparticles, mild neurotoxic effects, areas with mild neuronal damage and gliosis. The section of the hippocampus presented in the image provides further insights into the therapeutic potential of collagen nanoparticles, with mild clustering of damaged cells suggests significant neuronal loss, and inflammation. (Figure 26,27). The histological section of brain tissue shown in the image provides an examination of the effects of aluminum chloride (AlCl3) toxicity and subsequent treatment with silymarin nanoparticles, Brain showing cerebrum with mild congested meninges, mild degeneration in neurons with perineuronal and perivascular edema. Hippocampus showing the pyramidal layer with mild degeneration in neurons, with areas where glial cells have proliferated, with noticeable reduction in gliosis and maintaining a higher neuronal density is crucial for preserving the cognitive functions and structural integrity of the hippocampus (Figure 28,29).The section of the hippocampus from a rat induced with aluminium chloride (AlCl3) and treated with

nano collagen plus silymarin, reveals significant neuroprotective effects and structural preservation. The neurons exhibit more normal shapes and sizes, indicating that the combined treatment effectively mitigates the neurotoxic impact of AlCl3.The neuronal density in the hippocampus section is better preserved, with fewer signs of neuronal loss compared to untreated AlCl3-exposed sections, significant anti-inflammatory properties indicated by reducing gliosis (Figure 30,31).

Scores of degenerations in brain and hippocampus

In case of control negative group, providing a baseline of normal brain histology without any induced neurotoxic damage. While in case of AlCl3 group results show profound neurotoxic effects of AlCl3, characterized by widespread neuronal damage, structural disintegration of the pyramidal layer, and vascular congestion in the cerebrum. silymarin treated group demonstrates considerable neuroprotection. No neuronal degeneration with mild pyramidal layer degeneration and mild cerebrum congestion indicating partial protection against vascular damage. In the collagen-treated group, moderate neuronal degeneration and pyramidal layer degeneration, along with notable cerebrum congestion. These results indicate that collagen provides some degree of neuroprotection but is less effective than silymarin in preventing neuronal and pyramidal layer degeneration and cerebrum congestion. While The use of silymarin nanoparticles significantly enhances neuroprotection. Minimal neuronal degeneration with mild pyramidal layer degeneration, along with reduced cerebrum congestion, resulting in more robust protection against AlCl3-induced damage. The group treated with silymarin collagen nanoparticles exhibits no neuronal degeneration, no degeneration of the pyramidal layer , and no cerebrum congestion .The combined treatment with silymarin and collagen in nanoparticle form appears to synergistically enhance neuroprotective effects, effectively preserving neuronal integrity, maintaining the structural organization of the pyramidal layer, and preventing vascular congestion in the cerebrum and protection against AlCl3-induced neurotoxicity.

Discussion

Alzheimer’s disease (AD) has recently attracted significant scientific interest and public awareness in modern biomedicine. It was virtually unknown to the public approximately four decades ago(Hampel et al., 2016; Selkoe & Hardy, 2016) .Notwithstanding the notable rise in The incidence of Alzheimer’s disease throughout the last hundred years, a definitive cure for this condition has yet to be discovered,(Association, 2016).

AD is an advanced neurodegenerative condition that is influenced by multiple factors and typically affects adults in the middle to later stages of life. The hallmark symptom of Alzheimer’s disease is the gradual deterioration of memory function, impairment of episodic memory was a notable symptom observed early in the course of neurodegenerative cognitive disorder, alongside progressive mental decline and fluctuations in function and behavior, which significantly impacted individuals' capacity to achieve everyday tasks (Anand et al., 2022; Anand, Patience, Sharma, & Khurana, 2017). The hippocampus, a vital brain region responsible for specific dimensions of learning and memory, is considered one of the most liable areas during the early stages of Alzheimer's disease and additional neurodegenerative diseases. (Raji, Torosyan, & Silverman, 2020).

Research has shown that exposure to environmental heavy metals has a significant impact on brain development , It is connected with neurodegenerative conditions like Alzheimer’s disease (AD) and Parkinson’s disease (PD).(Shvachiy, Geraldes, & Outeiro, 2023). Aluminum is abundant metal which have been associated with the onset of cognitive impairment and neurodegenerative diseases.(Tomljenovic, 2011), It also caused severe neurotoxicity by functionally modifying the blood-brain barrier, affecting cholinergic and noradrenergic neurotransmission, elevating lipid peroxidation and free radical formation, and affecting phosphoinositide metabolism and

protein phosphorylation.(Said, EL-Tahawey, Elsayed, Shousha, & Elassal, 2013).

Silymarin is a highly promising natural compound originating from the fruits and seeds of the milk thistle plant (Silybum marianum), and it containing flavonolignans like silydianin, silybin, silychristin, and isosilybin. (Qavami, NAGHDI, Labbafi, & Mehrafarin, 2013). SM has been regarded as one of the most effective treatments for various liver conditions, as alcoholic liver disease, acute and chronic viral hepatitis, and toxins-related liver damage. (Abenavoli, Capasso, Milic, & Capasso, 2010). Over the past recent period, SM has gained significance as a compound with neuroprotective properties attributed to its antioxidant and anti-inflammatory characteristics within the central nervous system and its capacity to cross the blood-brain barrier, research has shown that silymarin exerts neuroprotective effects in experimental models of ischemia, dementia, and Alzheimer's disease. (Aboelwafa et al., 2020; Raza).

This study has confirmed the feasibility of producing valuable nanoparticles using fish scale-skin collagen, a development that could facilitate the achievement of long-term sustainability of marine resources and drive innovation in the field of nanotechnology SEM and TEM analyses demonstrated a uniform distribution of particles, indicating successful encapsulation of silymarin within the collagen-based nanoparticles.

This investigation was designed to assess the neuroprotective potential of nano-silymarin, developed by encapsulating silymarin Integrated within a collagen-based polymeric nanoparticle drug delivery system. DLS, SEM, and TEM analyses demonstrated the successful conjugation of silymarin to collagen nanoparticles and revealed their Size distribution of the particles and polydispersity. The observed uniformity and smooth surface morphology ensure reliable performance in targeted delivery systems and other advanced biomedical applications. (Elzoghby, Elgohary, & Kamel, 2015) Overall, the FTIR spectrum confirmed that the silymarin–collagen-loaded nanoparticles were successfully synthesized. (Zhang et al., 2022).

We evaluated The in vitro release profiles of both free silymarin and silymarin-loaded nanoparticles over a 48-hour period. These release profiles are essential for assessing the therapeutic potential and stability of the delivery system. Notably, free silymarin exhibited a significantly faster release rate than the nanoparticulate formulation. (Khalil et al., 2024). Free silymarin became available in solution more quickly, which may produce faster but less controlled therapeutic effects. In contrast, the silymarin-loaded nanoparticles exhibited a slower, more controlled release into phosphate buffer at physiological pH (7.4).(Macit, Duman, Cumbul, Sumer, & Macit, 2023) This controlled-release profile is beneficial because it delivers the drug steadily over an extended period, helping to maintain therapeutic levels and reduce dosing frequency. The slower release from the nanoparticles likely results from their encapsulating matrix, which modulates diffusion. In this system, the silymarin must diffuse through the nanoparticle's matrix barrier, thereby regulating its release into the surrounding medium (Bilia, Piazzini, & Bergonzi, 2020). The nanoparticles' controlled, sustained release of silymarin highlights their potential for therapies that require maintenance of consistent drug concentrations (Yang et al., 2013).

In our present investigation, the cytotoxicity of both free silymarin and silymarin-loaded nanoparticles was assessed in WI-38 normal lung cells using the MTT assay. The IC_{50} for free silymarin was approximately 125 µg/mL, indicating a 50% reduction in cell viability at that concentration. In contrast, the IC_{50} for the nanoparticle formulation was significantly higher, reflecting its lower cytotoxicity, that also report by (Awad et al., 2022) so, when comparing the two forms of Silymarin, it is evident that at every concentration level, the cell viability is higher for Silymarin nanoparticles than for free Silymarin as reported by (Kesharwani et al., 2020) , The nanoparticles exhibited reduced toxicity to the cells, and the cells remained more viable when exposed to the nanoparticles, as opposed to their pre-existing state, suggesting

a lower cytotoxic effect of the nanoparticle formulation.(Rathore et al., 2020). Treating the surface with coating materials would decrease the material's reactivity and in turn decrease its cytotoxic potential, Collagen nanoparticles without additives demonstrated the lowest toxicity, even at the highest concentration that was tested. (Anwar et al., 2022)

Both Silymarin and collagen nanoparticles showed a dose-dependent increase in haemolysis, but Silymarin nanoparticles were more prone to causing haemolysis at higher concentrations. The proposed use may be influenced by the fact that, although nanoparticles may provide several benefits, including enhanced bioavailability, their capacity to induce haemolysis at higher doses requires thorough evaluation. (Piazzini et al., 2019).

Research conducted in a living organism found that in a passive avoidance test, the most significant improvement occurred in the group that received silymarin collagen nanoparticles, with response times most similar to those of a control group that did not receive treatment. The combination of silymarin and collagen in a nanoparticle format appeared to result in a synergistic effect, offering significant neuroprotection and cognitive benefits against neurotoxicity induced by AlCl3. (Kumar et al., 2019).

Silymarin treatment led to a partial reversal of these effects, with mixed outcomes observed from collagen treatment showing some improvement. Treatment with silymarin nanoparticles consistently improved outcomes in rats, demonstrating a significant level of protection and recovery from the damage caused by AlCl3, as described by (Liang et al., 2010; Zorkina et al., 2020) .

The outcomes of the current study demonstrated that administration of aluminum chloride caused a progressive decline in spatial memory, judged by the Morris water maze test, as well as in retention memory, evaluated using the passive avoidance test , In experimental conditions, administering aluminum chloride to rats caused learning deficits during the Morris water maze task. (Lakshmi, Sudhakar, & Prakash, 2015). The observed phenomenon may be attributed to aluminum's capacity to disrupt downstream effector molecules that are essential for longstanding potentiation. This disturbance likely contributes to the resulting memory diminishing and neurobehavioral deficits. That agreed with (Shunan, Yu, Guan, & Zhou, 2021). The most notable recovery was observed in the silymarin collagen nanoparticles group, where performance metrics closely match those of the control negative group, that agreed with (Tian et al., 2019) that reported that indicated a synergistic effect of silymarin and collagen when delivered as nanoparticles(Shunan et al., 2021).Catalase is one of the fastest enzymes known, with each molecule able to Catalyze the conversion of millions of hydrogen peroxide molecules into water and oxygen per second. (Althiyabi, Eid, & Almukadi; Rathore et al., 2020)

In the existing experiment, application of $AlCl_3$ brought significant oxidative stress in hippocampal tissues, as evidenced by augmented levels of lipid peroxidation (LPO) and nitric oxide (NO), along with decreased levels of glutathione (GSH). Additionally, The values of catalase (CAT), glutathione peroxidase (GPx), and superoxide dismutase (SOD) were impaired, consistent with oxidative stress commonly associated with Alzheimer's disease.(Gravandi et al., 2024). Previous studies by several authors have confirmed that sub-chronic exposure to $AlCl_3$ brings oxidative damage in brain tissues (Agrawal et al., 2024). The recent study demonstrated that collagen treatment alone significantly reduced TBARS levels in $AlCl_3$-induced Alzheimer's groups, suggesting its potent antioxidant activity—potentially greater than that of silymarin or silymarin nanoparticles(García-Muñoz, Victoria-Montesinos, Ballester, Cerdá, & Zafrilla, 2024; Stoia & Oancea, 2022), The study also reported that silymarin treatment effectively reduced NO levels, highlighting its strong antioxidant potential. Additionally, it significantly improved GSH levels, indicating effective mitigation of oxidative stress. In contrast, the nanoparticle form of silymarin showed limited effectiveness in lowering NO levels.(Perez-Araluce et al., 2024) , The group treated with silymarin-loaded collagen

nanoparticles revealed no statistically significant variation in GSH amount as opposed to the control group, indicating height effectiveness likely attributed to improved bioavailability. (Bansal et al., 2023) , Moreover, this treatment was the most effective in enhancing SOD activity. Both silymarin and silymarin-loaded collagen nanoparticles were effective in restoring catalase activity to near-normal levels(Prasad & Prasad, 2019) , Treatment with silymarin nanoparticles resulted in the most significant increase of glutathione (GSH), glutathione peroxidase (GPx), catalase (CAT), and superoxide dismutase (SOD) activities, highlighting its potential as an effective treatment for oxidative damage in Alzheimer's disease. Additionally, the combination of silymarin with collagen nanoparticles showed considerable improvement, indicating possible synergistic effects in mitigating oxidative stress related to Alzheimer's disease (Haddadi et al., 2024; Moghaddam, Sangdehi, Ranjbar, & Hasantabar, 2020), In our study, silymarin (SM) alone significantly reduced oxidative damage induced by AlCl3. SM is known for its potent antioxidant activity, mainly attributed to its capacity to neutralize free radicals, thereby inhibiting lipid peroxidation in cellular membranes (Li, Sun, Liu, Zhao, & Shao, 2017).

The biochemical results were supported by histopathological findings. The histopathological characteristics of Neurodegenerative dementia included the ongoing deterioration of specific brain neurons. (K. Ravi, Paidas, Saad, & Jayakumar, 2021; S. K. Ravi, Ramesh, Mundugaru, & Vincent, 2018), The hippocampus was highly susceptible to neuronal damage . The hippocampus, which plays a crucial role in memory functions, is the first region to be affected by the degenerative process in individuals with Alzheimer's disease. (E Abdel Moneim, 2015; Nairuz, Heo, & Lee, 2024).

The histopathological changes observed in the hippocampal sections of rats treated with AlCl3 included neuronal damage, vacuolation, reduced neuronal density, intracytoplasmic inclusions, potential gliosis, and disorganization of layers. These alterations highlight the significant neurotoxic effects of aluminum chloride, which compromise hippocampal structure and function, mirroring the clinical features of neurodegenerative disorders, that agreed with (Bettio, Rajendran, & Gil-Mohapel, 2017). This neuronal loss plays a critical contribution in the advancement of neurodegenerative disorders (Jurkowski et al., 2020). These inclusions were frequently observed across multiple neurodegenerative diseases and interfered with regular cellular functions. The presence of them in this section suggested that exposure to AlCl3 might cause pathological alterations similar to those observed in diseases such as Alzheimer's.

Additionally, potential signs of gliosis were observed in the section. Gliosis involves an increase in glial cells due to neuronal damage and represents the brain's attempt to repair and protect the neural environment, that reported by (Pekny & Pekna, 2014). Finally, noticeable disorders were observed in the hippocampal layers, particularly in the CA1 and CA3 regions, which are essential for synaptic transmission and plasticity that agreed with (Dai et al., 2015) .

In the silymarin-treated rats, the sections displayed some neurons with signs of shrinkage and irregular shapes, indicating residual effects of AlCl3 toxicity. However, the extent of this damage was reduced compared to the AlCl3-exposed sections. This suggests that silymarin helped preserve neuronal shape, reduce cellular stress, and maintain neuronal integrity, that agreed with (Aboelwafa et al., 2020) The findings demonstrated that silymarin significantly reduced neuronal damage, vacuolation, neuronal loss, and gliosis, while preserving neuronal morphology, density, and layer organization. This suggests that silymarin may help stabilize cellular membranes and prevent the breakdown of cellular components typically caused by AlCl3 exposure.(A. Karim et al., 2023). Moreover, the absence or reduction of intracytoplasmic inclusions and the diminished inflammatory response in this section suggest that silymarin may inhibit the accumulation of abnormal proteins or damaged cellular components within neurons.

that reported by (Abdullah, Nour, & Mansouri, 2022; Haddadi et al., 2020).

Collagen, being a key structural protein of the extracellular matrix, may also promote tissue repair, as evidenced by the improved extracellular matrix structure and potential new tissue formation in the treated areas reported by (Arun, Malrautu, Laha, Luo, & Ramakrishna, 2021) . Treatment with collagen appeared to offer a neuroprotective effect against AlCl3-induced damage. Areas within the histological section that exhibited relatively preserved neuronal structures, compared to untreated regions, suggested that collagen nanoparticles help mitigate neuronal damage. Additionally, there was evidence of reduced gliosis, as indicated by fewer microglia and astrocytes, pointing to a decrease in inflammation. Collagen therapy may also contribute to regenerating the Brain endothelial barrier, although the presence of slight hemorrhage highlights the extent of damage caused by AlCl3. reported by (Rathore et al., 2020; Rehman et al., 2024).

Histopathological analysis of the hippocampus from rats treated with AlCl3 and silymarin nanoparticles revealed a notable neuroprotective effect. The nanoparticles enhanced the efficacy of silymarin, resulting in improved preservation of neuronal structure, reduced vacuolation, increased neuronal density, better layer organization, fewer intracytoplasmic inclusions, and decreased gliosis. These findings agreed with(Kabir et al., 2014), Histological examination of a rat's brain following treatment with silymarin-collagen nanoparticles and AlCl3 revealed significant neuroprotective effects. The combination treatment not only prevented the formation of intracytoplasmic inclusions but also successfully maintained neuronal density, reduced vacuolation, and preserved neuronal structure. Furthermore, it decreased gliosis, indicating potent anti-inflammatory effects, These findings agreed with (Rathore et al., 2020) . While silymarin alone provided notable neuroprotection, the comparative histological analysis revealed that its effectiveness was significantly enhanced when prepared as nanoparticles. Collagen alone offered a moderate level of protection, but the most significant neuroprotective benefits were observed when collagen was combined with silymarin in nanoparticle form. These results highlight how advanced nanoparticle drug delivery systems hold the possibility to improve the efficacy of neuroprotective medications, offering promising strategies to mitigate the neurodegenerative changes induced by aluminum exposure

Conclusion

Cytotoxicity results indicated that the Marine collagen loaded with silymarin nanoparticles exhibited biocompatibility with healthy cells, as such, could be utilized safely as carriers in pharmaceuticals, The evidence obtained in this study indicated that treatment with Marine collagen loaded with SM enhanced the therapeutic efficacy of SM in treatment of Alzheimer's disease by increasing its bioavailability and high efficacy in memory retention and learning. Using mullet fish scale collagen as a nanocarrier has no side effects due to its great biodegradability, brilliant biocompatibility, and low antigenicity.

5. References

Abdullah, F., Nour, N., & Mansouri, R. (2022). The Neuroprotective Effect of Lycopodium and Withania Somnifera on Alzheimer's Disease Induced by Aluminum Chloride in Rats. *European Online Journal of Natural and Social Sciences, 11*(3), pp. 852-861.

Abenavoli, L., Capasso, R., Milic, N., & Capasso, F. (2010). Milk thistle in liver diseases: past, present, future. *Phytotherapy research, 24*(10), 1423-1432.

Aboelwafa, H. R., El-Kott, A. F., Abd-Ella, E. M., & Yousef, H. N. (2020). The possible neuroprotective effect of silymarin against aluminum chloride-prompted Alzheimer's-like disease in rats. *Brain Sciences, 10*(9), 628.

Agrawal, M., Singhal, M., Semwal, B. C., Arora, S., Singh, B., Sikarwar, V., . . . Bhargva, S. (2024). Neuroprotective action of hordenine against the Aluminium Chloride (AlCl3) induced Alzheimer's diseases & associated memory impairment in experimental rats. *Pharmacological Research-Modern Chinese Medicine, 12*, 100492.

Althiyabi, N. N., Eid, B. G., & Almukadi, H. S. PROTECTIVE ACTIVITIES OF ALANTOLACTONE AGAINST THIOACETAMIDE-INDUCED LIVER INJURY IN MICE.
Anand, A., Khurana, N., Ali, N., AlAsmari, A. F., Alharbi, M., Waseem, M., & Sharma, N. (2022). Ameliorative effect of vanillin on scopolamine-induced dementia-like cognitive impairment in a mouse model. *Frontiers in Neuroscience, 16*, 1005972.
Anand, A., Patience, A. A., Sharma, N., & Khurana, N. (2017). The present and future of pharmacotherapy of Alzheimer's disease: A comprehensive review. *Eur J Pharmacol, 815*, 364-375.
Anwar, M. M., Shalaby, M. A., Saeed, H., Mostafa, H. M., Hamouda, D. G., & Nounou, H. (2022). Theophylline-encapsulated Nile Tilapia fish scale-based collagen nanoparticles effectively target the lungs of male Sprague–Dawley rats. *Scientific Reports, 12*(1), 4871.
Arun, A., Malrautu, P., Laha, A., Luo, H., & Ramakrishna, S. (2021). Collagen nanoparticles in drug delivery systems and tissue engineering. *Applied Sciences, 11*(23), 11369.
Association, A. s. (2016). 2016 Alzheimer's disease facts and figures. *Alzheimer's & Dementia, 12*(4), 459-509.
Awad, A., Shalaby, M., Batiha, G., Mady, R., AL-kuraishy, H. M., & Shaheen, H. M. (2022). Cytotoxicity Effect Assessment of Theophylline Loaded with Collagen Nanoparticles. *Damanhour Journal of Veterinary Sciences, 8*(2), 5-10.
Bansal, P., Sharma, V., Panwar, A., Kumar, R., Sharma, A., Ramniwas, S., . . . Sharma, A. K. (2023). Computational Docking Study of the Phytochemical Constituent, Silybin (Silybum marianum) against SARS-CoV-2 Omicron Variant Spike Glycoprotein: An In-silico Approach. *J Pure Appl Microbiol*.
Begines, B., Ortiz, T., Pérez-Aranda, M., Martínez, G., Merinero, M., Argüelles-Arias, F., & Alcudia, A. (2020). Polymeric nanoparticles for drug delivery: Recent developments and future prospects. *Nanomaterials, 10*(7), 1403.
Bettio, L. E., Rajendran, L., & Gil-Mohapel, J. (2017). The effects of aging in the hippocampus and cognitive decline. *Neuroscience & Biobehavioral Reviews, 79*, 66-86.
Bielawski, W., & Joy, K. (1986). Reduced and oxidised glutathione and glutathione-reductase activity in tissues of Pisum sativum. *Planta, 169*, 267-272.
Bilia, A. R., Piazzini, V., & Bergonzi, M. C. (2020). Nanotechnology Applications for Natural Products Delivery. *Sustainable Agriculture Reviews 44: Pharmaceutical Technology for Natural Products Delivery Vol. 2 Impact of Nanotechnology*, 1-46.
Chen, H., & Tappel, A. (1996). Protection by multiple antioxidants against lipid peroxidation in rat liver homogenate. *Lipids, 31*(1Part1), 47-50.
Chiu, Y.-C., Algase, D., Whall, A., Liang, J., Liu, H.-C., Lin, K.-N., & Wang, P.-N. (2004). Getting lost: directed attention and executive functions in early Alzheimer's disease patients. *Dementia and geriatric cognitive disorders, 17*(3), 174-180.
Cordaro, M., Cuzzocrea, S., & Crupi, R. (2020). An update of palmitoylethanolamide and luteolin effects in preclinical and clinical studies of neuroinflammatory events. *Antioxidants, 9*(3), 216.
Dai, Z., Yan, C., Li, K., Wang, Z., Wang, J., Cao, M., . . . Bi, Y. (2015). Identifying and mapping connectivity patterns of brain network hubs in Alzheimer's disease. *Cerebral cortex, 25*(10), 3723-3742.
Drotar, A., Phelps, P., & Fall, R. (1985). Evidence for glutathione peroxidase activities in cultured plant cells. *Plant science, 42*(1), 35-40.
E Abdel Moneim, A. (2015). Oxidant/antioxidant imbalance and the risk of Alzheimer's disease. *Current Alzheimer Research, 12*(4), 335-349.
Elzoghby, A. O., Elgohary, M. M., & Kamel, N. M. (2015). Implications of protein-and peptide-based nanoparticles as potential vehicles for anticancer drugs. *Advances in protein chemistry and structural biology, 98*, 169-221.
Ferrer, I. (2022). Alzheimer's disease is an inherent, natural part of human brain aging: An integrated perspective. *Free Neuropathology, 3*.
Gamache, J., Yun, Y., & Chiba-Falek, O. (2020). Sex-dependent effect of APOE on Alzheimer's disease and other age-related neurodegenerative disorders. *Disease Models & Mechanisms, 13*(8), dmm045211.
García-Muñoz, A. M., Victoria-Montesinos, D., Ballester, P., Cerdá, B., & Zafrilla, P. (2024). A Descriptive Review of the Antioxidant Effects and Mechanisms of Action of Berberine and Silymarin. *Molecules, 29*(19), 4576.
Gravandi, M. M., Hosseini, S. Z., Alavi, S. D., Noori, T., Sureda, A., Amirian, R., . . . Shirooie,

S. (2024). The Protective Effects of Pistacia Atlantica Gum in a Rat Model of Aluminum Chloride-Induced Alzheimer's Disease via Affecting BDNF and NF-kB. *Iranian Journal of Pharmaceutical Research: IJPR, 23*(1).
Haddadi, R., Eyvari-Brooshghalan, S., Makhdoomi, S., Fadaiie, A., Komaki, A., & Daneshvar, A. (2024). Neuroprotective effects of silymarin in 3-nitropropionic acid-induced neurotoxicity in male mice: Improving behavioral deficits by attenuating oxidative stress and neuroinflammation. *Naunyn-Schmiedeberg's Archives of Pharmacology, 397*(4), 2447-2463.
Haddadi, R., Shahidi, Z., & Eyvari-Brooshghalan, S. (2020). Silymarin and neurodegenerative diseases: Therapeutic potential and basic molecular mechanisms. *Phytomedicine, 79*, 153320.
Hampel, H., O'Bryant, S., Castrillo, J., Ritchie, C., Rojkova, K., Broich, K., . . . Dubois, B. (2016). Precision medicine-the golden gate for detection, treatment and prevention of Alzheimer's disease. *The journal of prevention of Alzheimer's disease, 3*(4), 243.
Jafari, H., Lista, A., Siekapen, M. M., Ghaffari-Bohlouli, P., Nie, L., Alimoradi, H., & Shavandi, A. (2020). Fish collagen: Extraction, characterization, and applications for biomaterials engineering. *Polymers, 12*(10), 2230.
Jurkowski, M. P., Bettio, L., K. Woo, E., Patten, A., Yau, S.-Y., & Gil-Mohapel, J. (2020). Beyond the hippocampus and the SVZ: adult neurogenesis throughout the brain. *Frontiers in cellular neuroscience, 14*, 576444.
Kabir, N., Ali, H., Ateeq, M., Bertino, M. F., Shah, M. R., & Franzel, L. (2014). Silymarin coated gold nanoparticles ameliorates CCl 4-induced hepatic injury and cirrhosis through down regulation of hepatic stellate cells and attenuation of Kupffer cells. *RSC Advances, 4*(18), 9012-9020.
Karim, A., Anwar, F., Saleem, U., Fatima, S., Ismail, T., Obaidullah, A. J., . . . Khan, H. (2023). Administration of α-lipoic acid and silymarin attenuates aggression by modulating endocrine, oxidative stress and inflammatory pathways in mice. *Metabolic Brain Disease, 38*(7), 2255-2267.
Karim, N., Khan, H., Khan, I., Guo, O., Sobarzo-Sánchez, E., Rastrelli, L., & Kamal, M. A. (2020). An increasing role of polyphenols as novel therapeutics for Alzheimer's: A review. *Medicinal chemistry, 16*(8), 1007-1021.
Kawahara, M., Tanaka, K.-i., & Kato-Negishi, M. (2021). Neurotoxicity of aluminum and its link to neurodegenerative diseases. *Metallomics Research, 1*(1), rev-47-rev-65.
Kesharwani, S. S., Jain, V., Dey, S., Sharma, S., Mallya, P., & Kumar, V. A. (2020). An overview of advanced formulation and nanotechnology-based approaches for solubility and bioavailability enhancement of silymarin. *Journal of Drug Delivery Science and Technology, 60*, 102021.
Khalil, M. S., Khan, I., Khan, F. A., Shireen, F., Zahoor, M., Azam, S., . . . Bari, A. (2024). Preparation of silymarin-loaded zein polysaccharide core–shell nanostructures and evaluation of their biological potentials. *Green Processing and Synthesis, 13*(1), 20240002.
Kumar, N., Rai, A., Reddy, N. D., Shenoy, R. R., Mudgal, J., Bansal, P., . . . Sharma, N. (2019). Improved in vitro and in vivo hepatoprotective effects of liposomal silymarin in alcohol-induced hepatotoxicity in Wistar rats. *Pharmacological reports, 71*(4), 703-712.
Lakshmi, B., Sudhakar, M., & Prakash, K. S. (2015). Protective effect of selenium against aluminum chloride-induced Alzheimer's disease: behavioral and biochemical alterations in rats. *Biological trace element research, 165*, 67-74.
Li, L., Sun, H.-y., Liu, W., Zhao, H.-y., & Shao, M.-l. (2017). Silymarin protects against acrylamide-induced neurotoxicity via Nrf2 signalling in PC12 cells. *Food and Chemical Toxicology, 102*, 93-101.
Liang, J., Pei, X., Zhang, Z., Wang, N., Wang, J., & Li, Y. (2010). The protective effects of long-term oral administration of marine collagen hydrolysate from chum salmon on collagen matrix homeostasis in the chronological aged skin of Sprague-Dawley male rats. *Journal of food science, 75*(8), H230-H238.
Liza, M. M., Roy, S., Iktidar, M. A., Chowdhury, S., & Sharif, A. B. (2024). Nutritional status, dietary habits, and their relation to cognitive functions: A cross-sectional study among the school aged (8–14 years) children of Bangladesh. *PloS one, 19*(5), e0304363.
Lo, S., & Fauzi, M. B. (2021). Current update of collagen nanomaterials—fabrication, characterisation and its applications: A review. *Pharmaceutics, 13*(3), 316.

Macit, M., Duman, G., Cumbul, A., Sumer, E., & Macit, C. (2023). Formulation development of Silybum marianum seed extracts and silymarin nanoparticles, and evaluation of hepatoprotective effect. *Journal of Drug Delivery Science and Technology, 83*, 104378.

Mahapatra, S., Mohanty, R., Dehury, L., Kumari, M. M., Mohanty, I., Mishra, I., & Panigrahi, G. (2020). Evaluate the anti-Anxiety, anti-convulsant and CNS depressant activities of ethanolic extracts of leaves of Pongamia pinnata. *Research Journal of Pharmacy and Life Sciences, 2020*, 98-108.

Mayer, R., Veronikas, S., & Shaughnessy, M. F. (2005). An interview with Richard Mayer. *Educational Psychology Review*, 179-189.

Meyerholz, D. K., & Beck, A. P. (2018). Principles and approaches for reproducible scoring of tissue stains in research. *Laboratory investigation, 98*(7), 844-855.

Moghaddam, A. H., Sangdehi, S. R. M., Ranjbar, M., & Hasantabar, V. (2020). Preventive effect of silymarin-loaded chitosan nanoparticles against global cerebral ischemia/reperfusion injury in rats. *Eur J Pharmacol, 877*, 173066.

Montgomery, H., Dymock, J. F., & Thom, N. (1962). The rapid colorimetric determination of organic acids and their salts in sewage-sludge liquor. *Analyst, 87*(1041), 949-955.

Nairuz, T., Heo, J.-C., & Lee, J.-H. (2024). Differential Glial Response and Neurodegenerative Patterns in CA1, CA3, and DG Hippocampal Regions of 5XFAD Mice. *International Journal of Molecular Sciences, 25*(22), 12156.

Nandi, A., & Chatterjee, I. (1988). Assay of superoxide dismutase activity in animal tissues. *Journal of biosciences, 13*, 305-315.

Pekny, M., & Pekna, M. (2014). Astrocyte reactivity and reactive astrogliosis: costs and benefits. *Physiological reviews, 94*(4), 1077-1098.

Perez-Araluce, M., Jüngst, T., Sanmartin, C., Prosper, F., Plano, D., & Mazo, M. M. (2024). Biomaterials-based antioxidant strategies for the treatment of oxidative stress diseases. *Biomimetics, 9*(1), 23.

Piazzini, V., D'Ambrosio, M., Luceri, C., Cinci, L., Landucci, E., Bilia, A. R., & Bergonzi, M. C. (2019). Formulation of nanomicelles to improve the solubility and the oral absorption of silymarin. *Molecules, 24*(9), 1688.

Prasad, R., & Prasad, S. B. (2019). A review on the chemistry and biological properties of Rutin, a promising nutraceutical agent. *Asian J. Pharm. Pharmacol, 5*(1), 1-20.

Qavami, N., NAGHDI, B. H., Labbafi, M., & Mehrafarin, A. (2013). A review on pharmacological, cultivation and biotechnology aspects of milk thistle (Silybum marianum (L.) Gaertn.).

Raji, C. A., Torosyan, N., & Silverman, D. H. (2020). Optimizing use of neuroimaging tools in evaluation of prodromal Alzheimer's disease and related disorders. *Journal of Alzheimer's Disease, 77*(3), 935-947.

Rathore, P., Arora, I., Rastogi, S., Akhtar, M., Singh, S., & Samim, M. (2020). Collagen nanoparticle-mediated brain silymarin delivery: an approach for treating cerebral ischemia and reperfusion-induced brain injury. *Frontiers in Neuroscience, 14*, 538404.

Ravi, K., Paidas, M. J., Saad, A., & Jayakumar, A. R. (2021). Astrocytes in rare neurological conditions: Morphological and functional considerations. *Journal of Comparative Neurology, 529*(10), 2676-2705.

Ravi, S. K., Ramesh, B. N., Mundugaru, R., & Vincent, B. (2018). Multiple pharmacological activities of Caesalpinia crista against aluminium-induced neurodegeneration in rats: Relevance for Alzheimer's disease. *Environmental toxicology and pharmacology, 58*, 202-211.

Raza, S. NEUROPROTECTIVE EFFECT OF MEDICINAL HERBS ON CEREBRAL ISCHEMIA IN MALE WISTAR RATS.

Rehman, I. U., Park, J. S., Choe, K., Park, H. Y., Park, T. J., & Kim, M. O. (2024). Overview of a novel osmotin abolishes abnormal metabolic-associated adiponectin mechanism in Alzheimer's disease: Peripheral and CNS insights. *Ageing Research Reviews*, 102447.

Sahithi, B., Ansari, S., Hameeda, S., Sahithya, G., Prasad, D. M., & Lakshmi, Y. (2013). A review on collagen based drug delivery systems. *Indian Journal of Research in Pharmacy and Biotechnology, 1*(3), 461.

Said, U., EL-Tahawey, N., Elsayed, E., Shousha, W. G., & Elassal, A. (2013). Pomegranate Alleviates Oxidative Damage and Neurotransmitter Alterations in Rats Brain Exposed to Aluminum Chloride and/or Gamma Radiation. *Journal of Radiation Research and Applied Sciences, 6*(1), 69-87.

Sakurai, M., Sekiguchi, M., Zushida, K., Yamada, K., Nagamine, S., Kabuta, T., & Wada, K. (2008). Reduction in memory in passive avoidance learning, exploratory behaviour and synaptic plasticity in mice with a spontaneous deletion in the ubiquitin C-terminal hydrolase L1 gene. *European Journal of Neuroscience, 27*(3), 691-701.

Sathya, B., Balamurugan, K., Anbazhagan, S., Jeganathan, N., Vimalson, D. C., & Punitha, E. (2018). Neuropharmacological Effect of Aqueous Extract of Bauhinia tomentosa L. Leaves in Experimental Animal Models. *Int J Pharm Sci Rev Res, 49*(2), 78-84.

Selkoe, D. J., & Hardy, J. (2016). The amyloid hypothesis of Alzheimer's disease at 25 years. *EMBO molecular medicine, 8*(6), 595-608.

Shalaby, M., Agwa, M., Saeed, H., Khedr, S. M., Morsy, O., & El-Demellawy, M. A. (2020). Fish scale collagen preparation, characterization and its application in wound healing. *Journal of Polymers and the Environment, 28*, 166-178.

Shunan, D., Yu, M., Guan, H., & Zhou, Y. (2021). Neuroprotective effect of Betalain against AlCl3-induced Alzheimer's disease in Sprague Dawley Rats via putative modulation of oxidative stress and nuclear factor kappa B (NF-κB) signaling pathway. *Biomedicine & Pharmacotherapy, 137*, 111369.

Shvachiy, L., Geraldes, V., & Outeiro, T. F. (2023). Uncovering the Molecular Link Between Lead Toxicity and Parkinson's Disease. *Antioxidants & redox signaling, 39*(4-6), 321-335.

Solanki, R., & Patel, S. (2024). Protein nanocarriers for the delivery of phytoconstituents *Nanotechnology Based Delivery of Phytoconstituents and Cosmeceuticals* (pp. 229-264): Springer.

Stoia, M., & Oancea, S. (2022). Low-molecular-weight synthetic antioxidants: classification, pharmacological profile, effectiveness and trends. *Antioxidants, 11*(4), 638.

Tian, H., Ding, N., Guo, M., Wang, S., Wang, Z., Liu, H., . . . Jiang, J. (2019). Analysis of learning and memory ability in an Alzheimer's disease mouse model using the Morris water maze. *JoVE (Journal of Visualized Experiments)*(152), e60055.

Tomljenovic, L. (2011). Aluminum and Alzheimer's disease: after a century of controversy, is there a plausible link? *Journal of Alzheimer's Disease, 23*(4), 567-598.

Usman, M., Ahmad, M., Madni, A. U., Asghar, N., Akhtar, M., & Atif, M. (2009). In-vivo Kinetics of Silymarin (Milk Thistle) on healthy male volunteers. *Tropical Journal of Pharmaceutical Research, 8*(4).

Yang, K. Y., Hwang, D. H., Yousaf, A. M., Kim, D. W., Shin, Y.-J., Bae, O.-N., . . . Choi, H.-G. (2013). Silymarin-loaded solid nanoparticles provide excellent hepatic protection: physicochemical characterization and in vivo evaluation. *International journal of nanomedicine*, 3333-3343.

Zhang, Z., Li, X., Sang, S., McClements, D. J., Chen, L., Long, J., . . . Qiu, C. (2022). A review of nanostructured delivery systems for the encapsulation, protection, and delivery of silymarin: An emerging nutraceutical. *Food Research International, 156*, 111314.

Zorkina, Y., Abramova, O., Ushakova, V., Morozova, A., Zubkov, E., Valikhov, M., . . . Chekhonin, V. (2020). Nano carrier drug delivery systems for the treatment of neuropsychiatric disorders: Advantages and limitations. *Molecules, 25*(22), 5294.

Table 1, Passive avoidance test in different groups

Groups	Slowest rat	Fastest rat
Control negative (group I)	12 sec	40 sec
Control positive (ALCL3) (group II)	10 sec	37 sec
Silymarin (group III)	11 sec	40 sec
Collagen (group IV)	15 sec	46 sec
Silymarin nanoparticles (group V)	9 sec	33 sec
Silymarin collagen nanoparticles (group VI)	11 sec	22 sec

Table 2: Scores of degenerations in brain and hippocampus.

Histopathological lesion	**Degeneration of neuron**	**Degeneration of pyramidal layer**	**Congestion of cerebrum**
Control negative (group I)	—	—	—
Control positive (ALCL3) (group II)	+++	+++	+++
Silymarin (group III)	—	+	+
Collagen (group IV)	++	++	++
Silymarin nanoparticles (group V)	+	+	+
Silymarin collagen nanoparticles (group VI)	+	—	—

(−) no change, (+) mild change, (++) moderate change, (+++) severe change

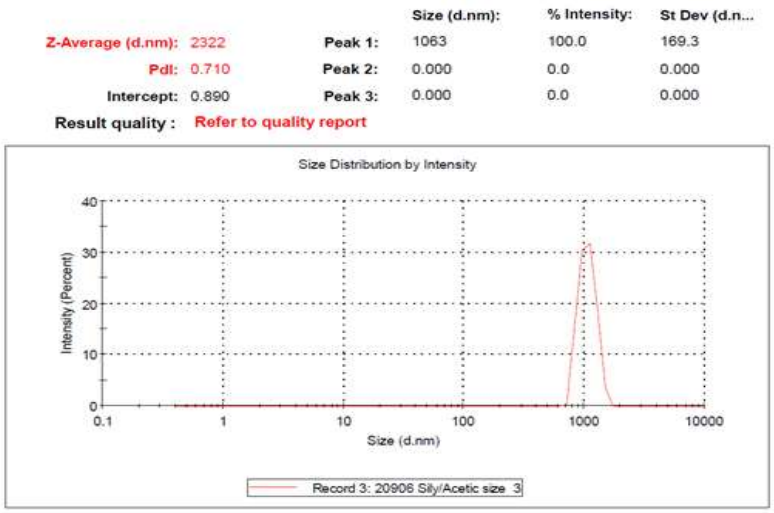

Figure 1: Dynamic light scattering pattern of silymarin

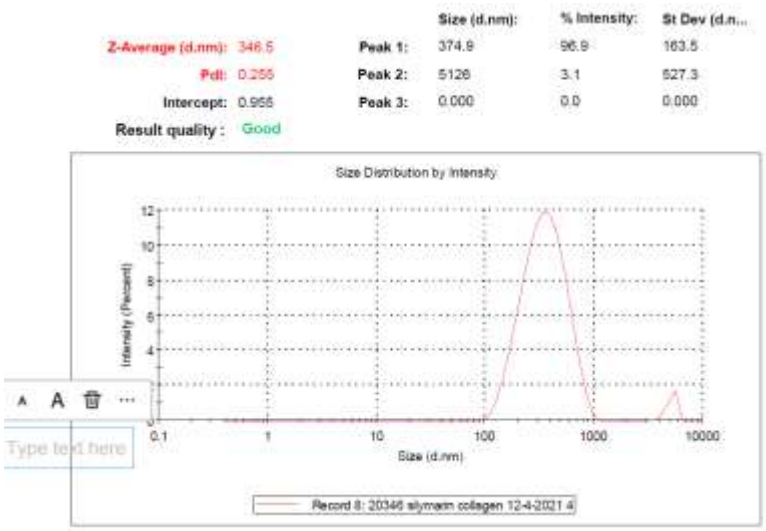

Figure 2: Dynamic light scattering pattern of silymarin collagen nanoparticles

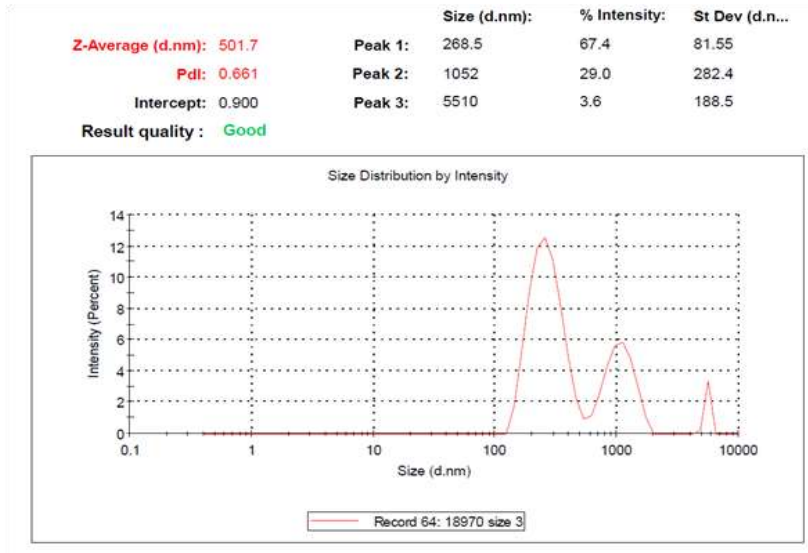

Figure 3: Dynamic light scattering pattern of silymarin nanoparticles

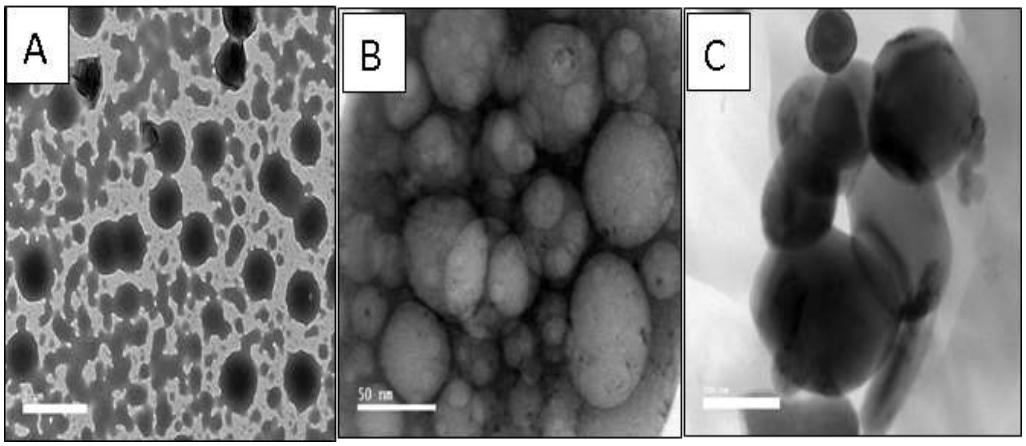

Figure 4: Transmission electron microscopy of silymarin(A), Collagen nanoparticles (B), silymarin loaded with collagen nanoparticles(C) .

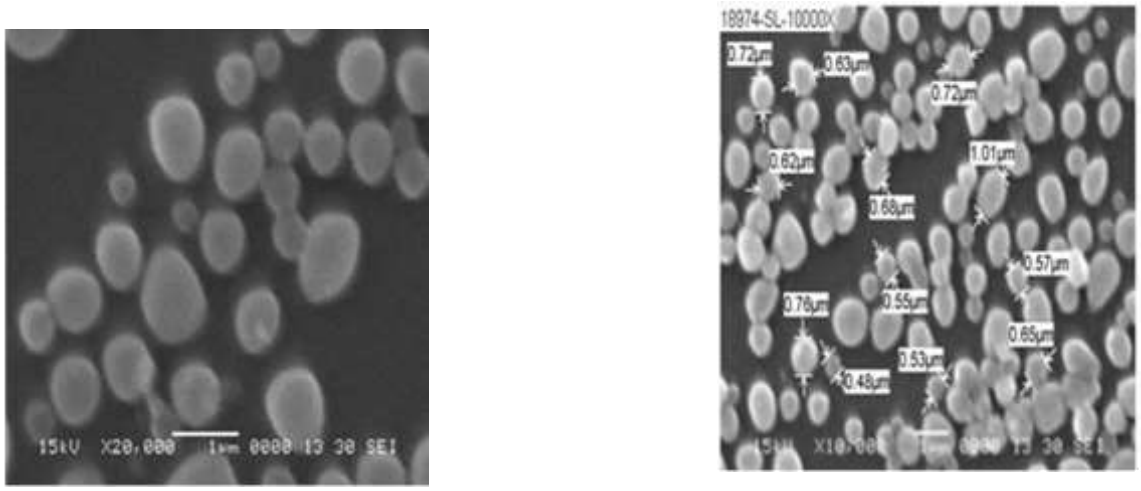

A ***B***

Figure 5: Scanning Electron Microscopy of silymaein (A) , silymarin nanoparticles (B) .

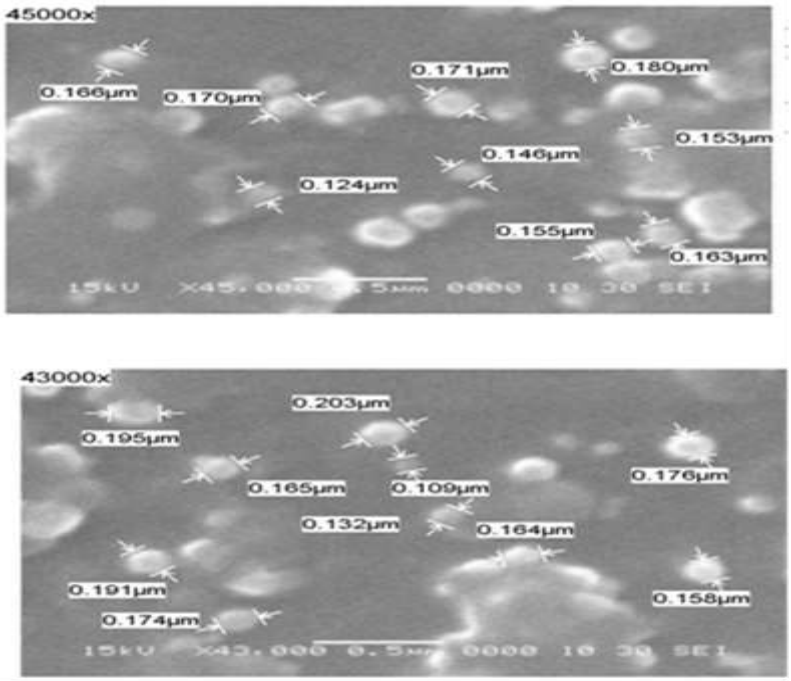

Figure 6: Scanning Electron Microscopy of silymarin loaded with collagen nanoparticles.

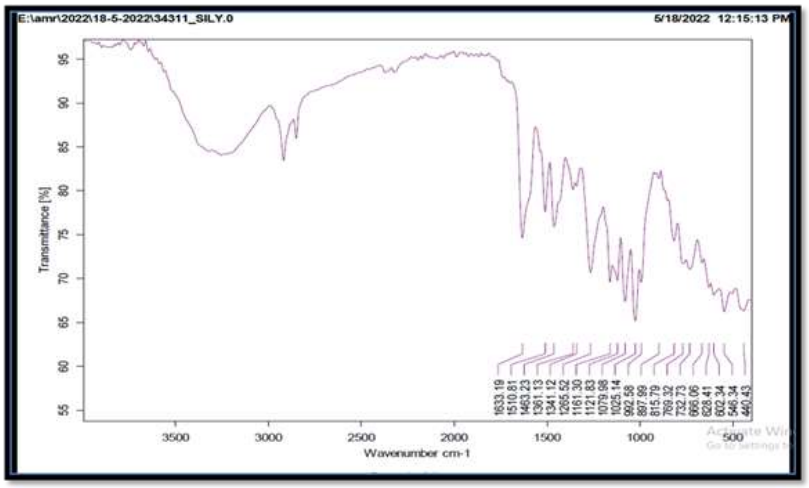

Figure 7: Fourier transform infrared (FT-IR)of silymarin

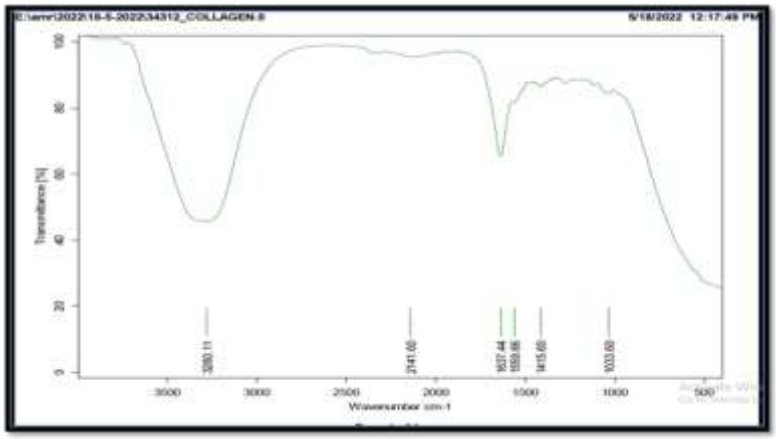

Figure 8: Fourier transform infrared (FT-IR)of collagen.

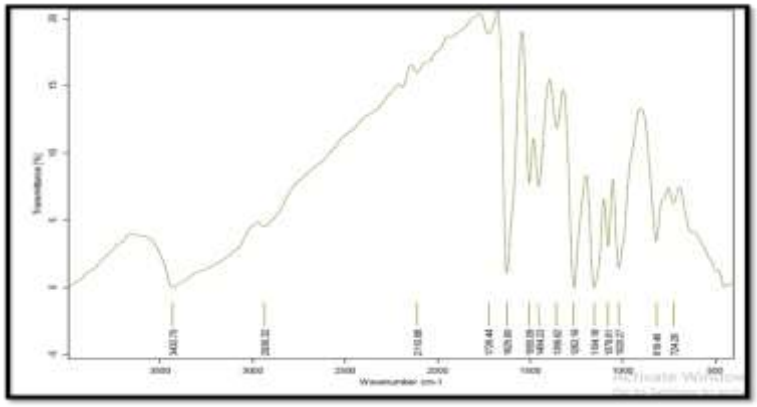

Figure 9: Fourier transform infrared (FT-IR)of silymarin nanoparticles

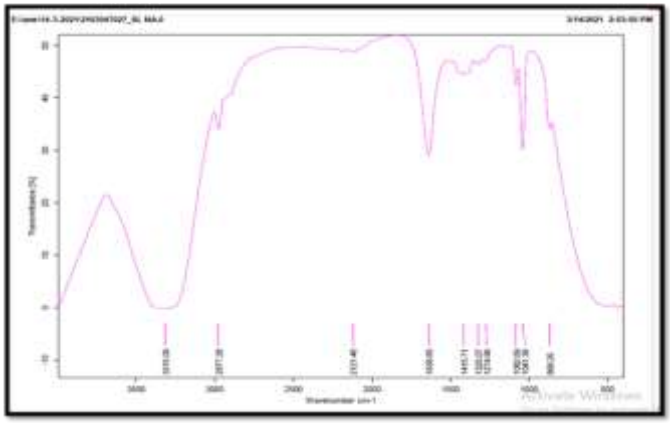

Figure 10: Fourier transform infrared (FT-IR)of silymarin collagen nanoparticles.

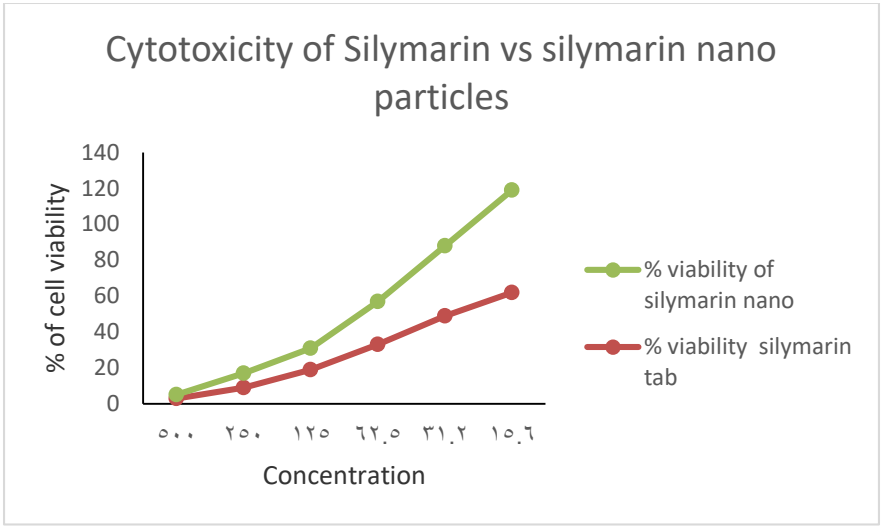

Figure 11: The cytotoxicity profile of silymarin and silymarin nanoparticles.

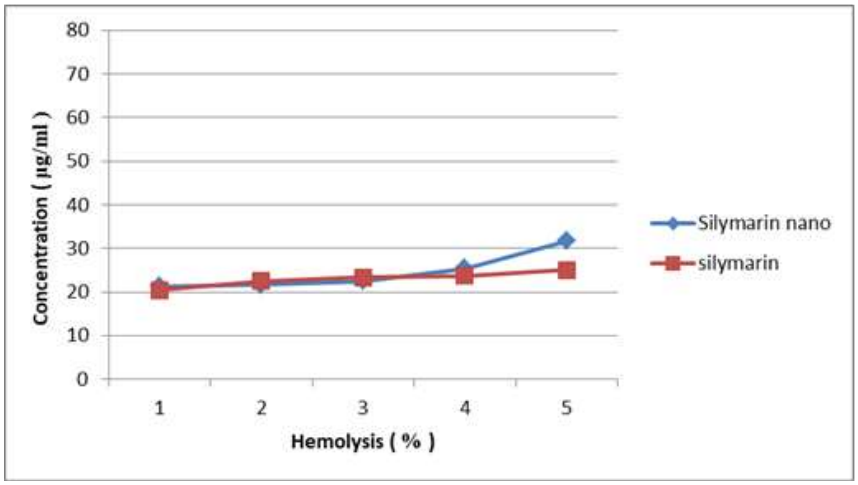

Figure 12: Hemolysis assay to test cytotoxicity

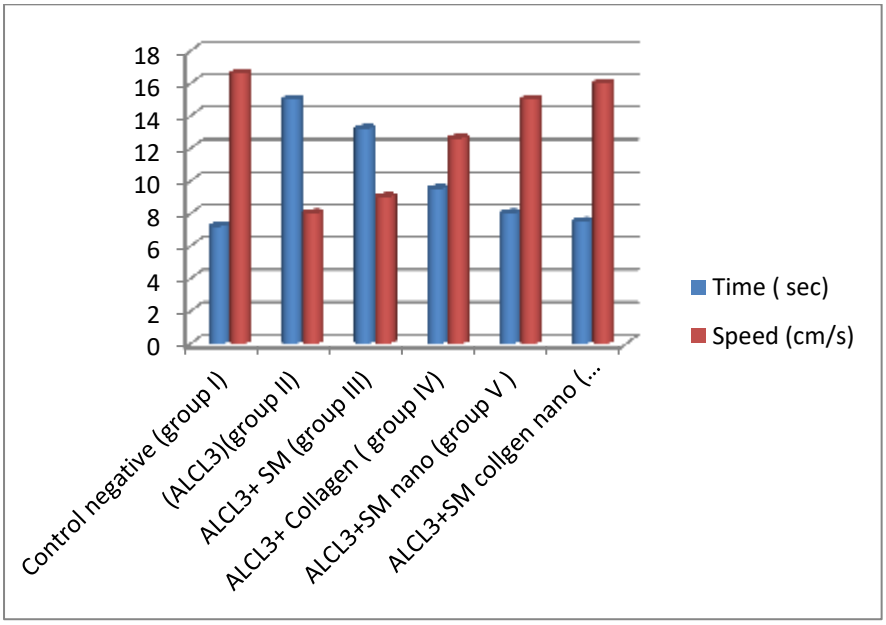

Figure 13 : showed comparison between control and all treated groups in water maze test(no. =3)

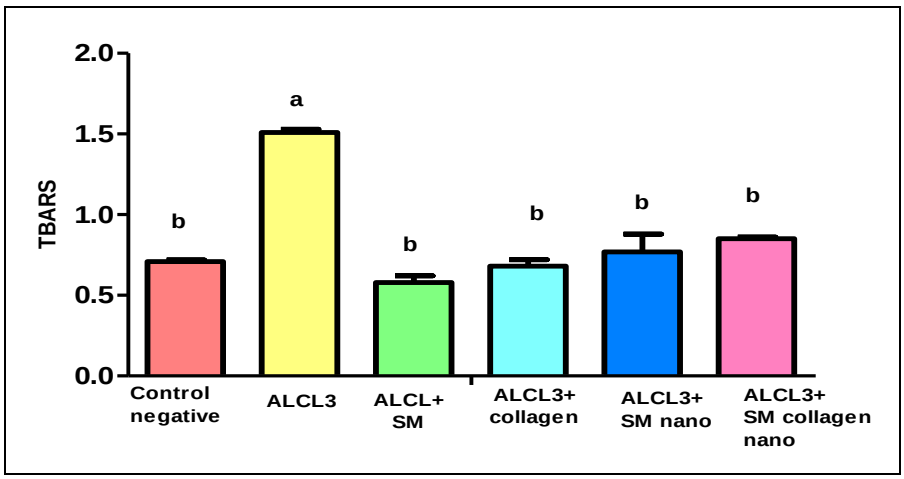

Figure 14: Showed changes in TBARS levels in studied groups. **(N=3)(M ± SE).**

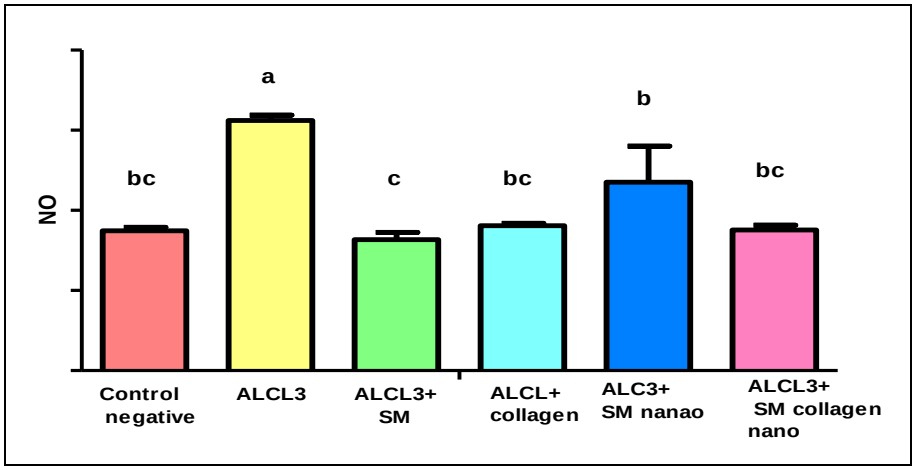

Figure 15: Showed changes in NO levels in studied groups. **(N=3) (M ± SE).**

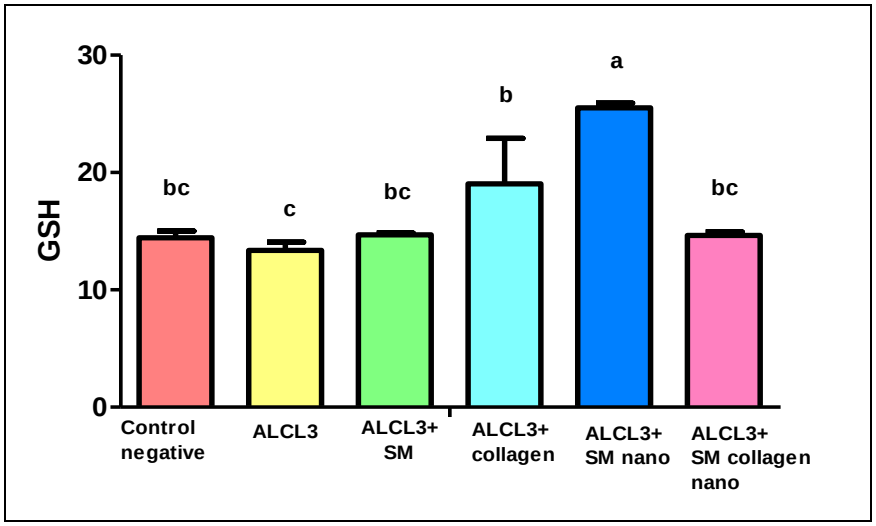

Figure 16: Showed changes in GSH levels in studied groups. **(N=3) (M ± SE).**

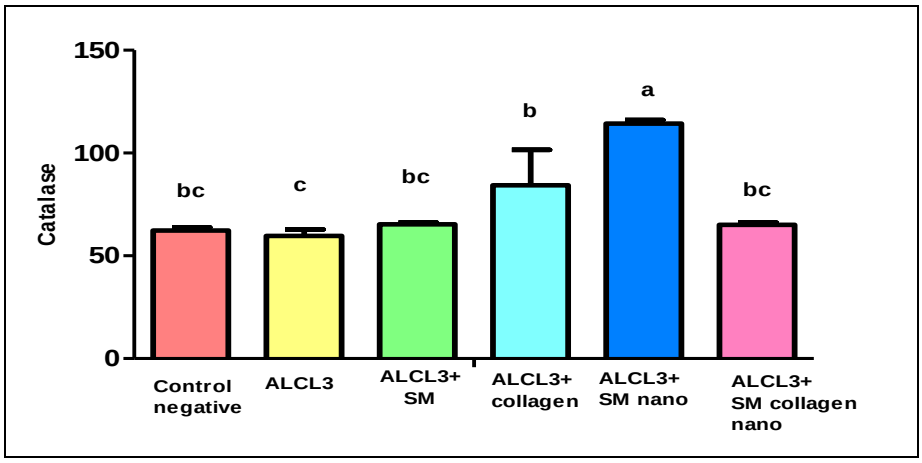

Figure 17: Showed changes in Catalase levels in studied groups. **(N=3) (M ± SE).**

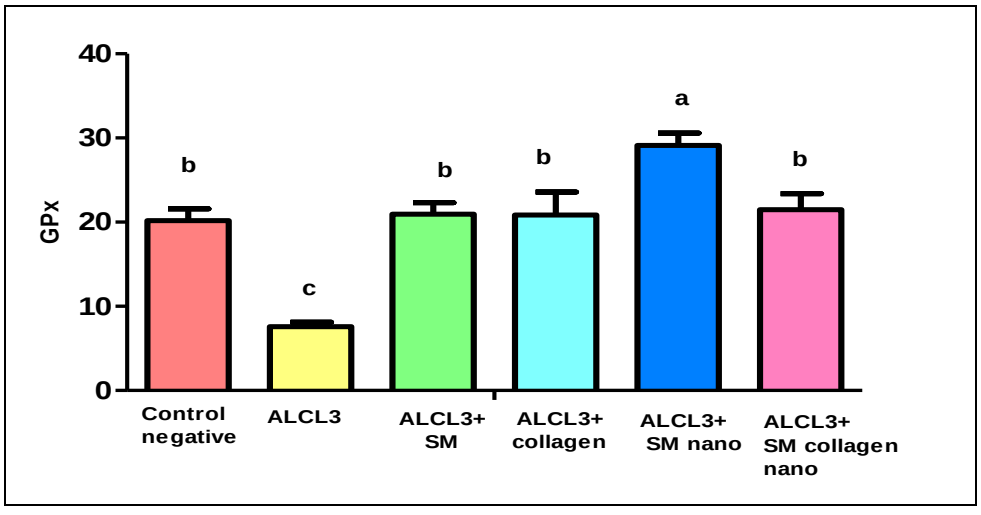

Figure 18: Showed changes in GPx levels in studied groups. **(N=3)(M ± SE).**

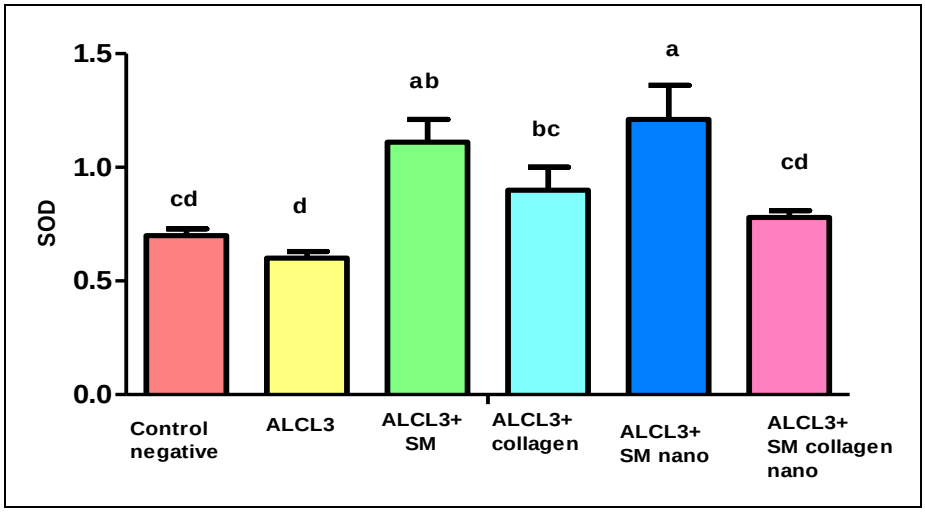

Figure 19: Showed changes in SOD levels in studied groups. **(N=3)(M ± SE).**

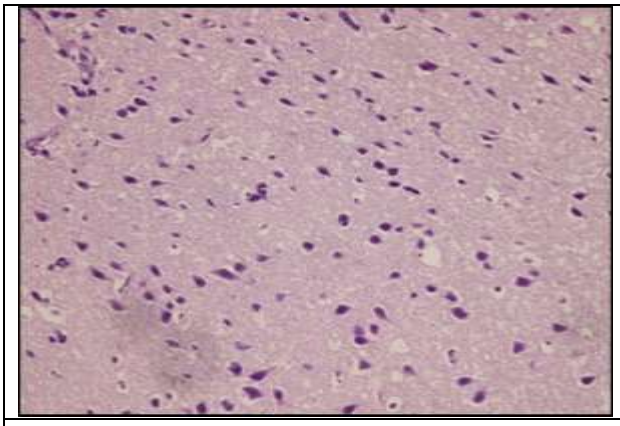

(Figure 20) brain showing cerebrum with normal meningeal layers, normal cerebral layer and normal neurons of control group

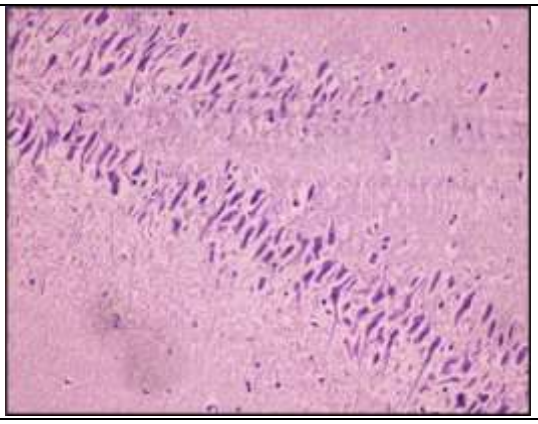

(Figure 21) Hippocampus showing normal pyramidal layer formed of densely packed neurons of control group

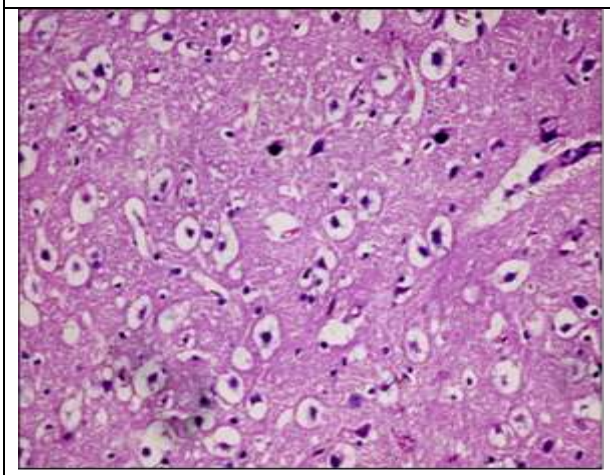

(Figure 22) Brain showing cerebrum with vacuolated and degenerated neurons of ALCL3 group

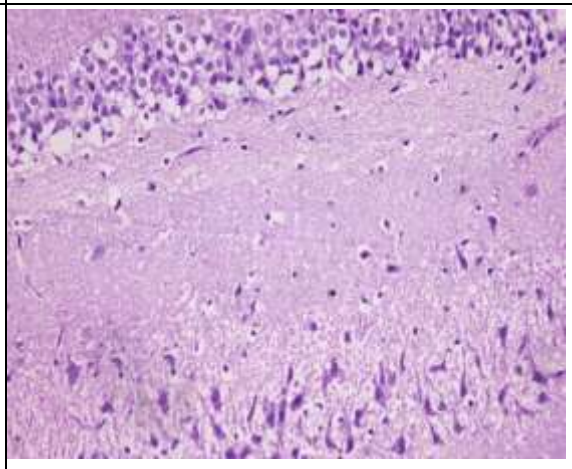

(Figure 23) Hippocampus showing neuropil vacuolation, degenerated neurons with pyknotic nuclei of ALCL3 group

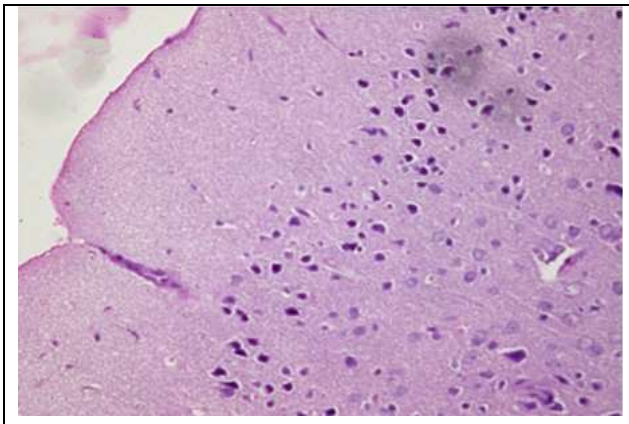

(Figure 24) Brain showing cerebrum with apparent normal neurons with mild degeneration and neuronophagia of silymarin group.

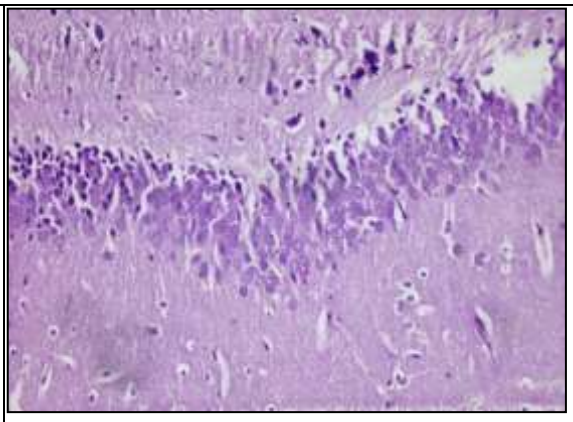

(Figure 25) Hippocampus showing the pyramidal layer with some degenerated neurons of silymarin group.

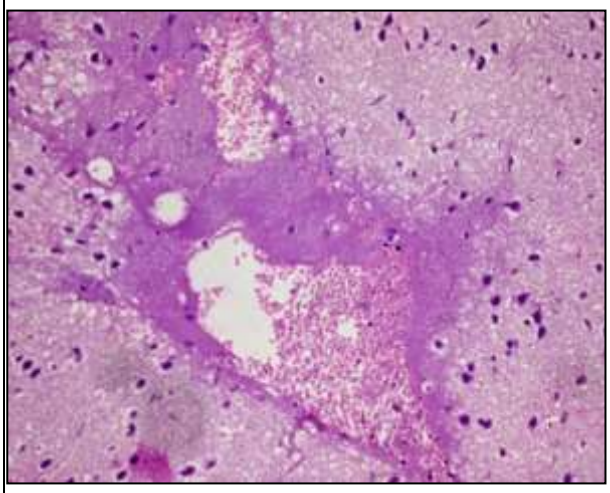

(Figure 26) Brain showing cerebrum with congested meninges, moderate degeneration in neurons with perineuronal and perivascular edema. notice the hemorrhagic patches of collagen group.

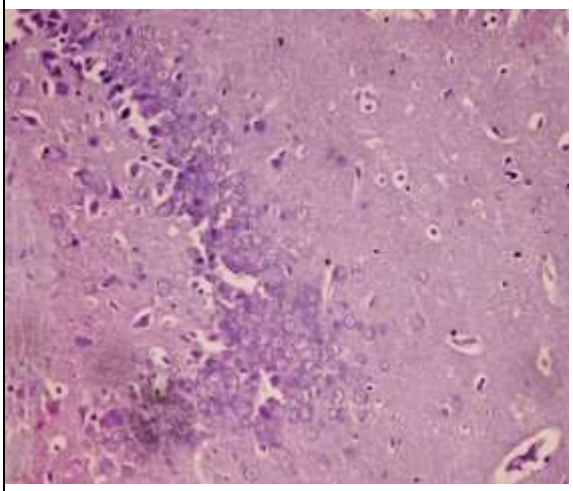

(Figure 27) Hippocampus showing the pyramidal layer with moderate degeneration in neurons of collagen group.

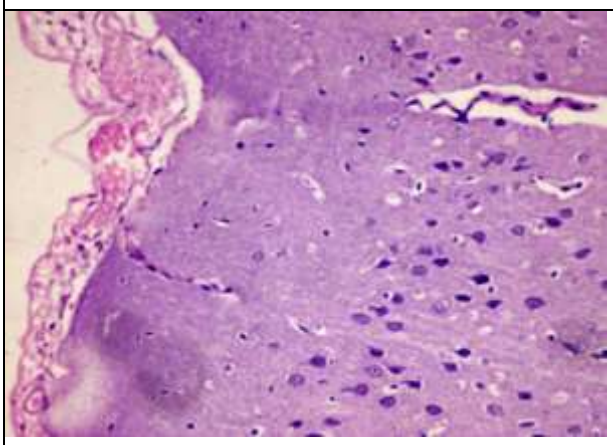

(Figure 28) brain showing cerebrum with congested meninges, mild degeneration in neurons with perineuronal and perivascular edema of silymarin nano group

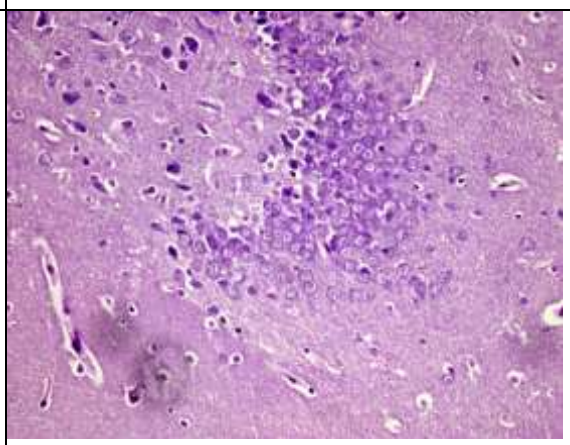

(Figure 29) Hippocampus showing the pyramidal layer with mild degeneration in neurons of silymarin nano group

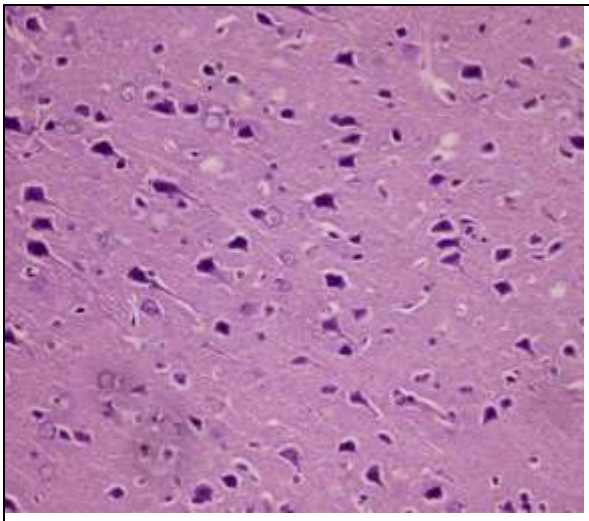

(Figure 30) brain showing cerebrum with apparent normal neurons of Silymarin collagen nanoparticles group

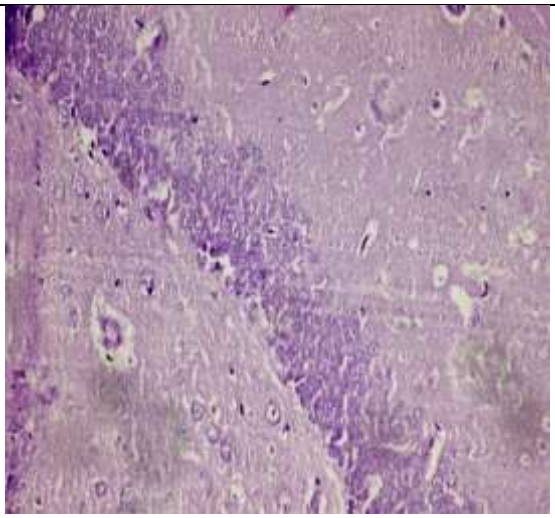

(Figure 31) Hippocampus showing apparent normal pyramidal layer with apparent normal neurons of Silymarin collagen nanoparticles group